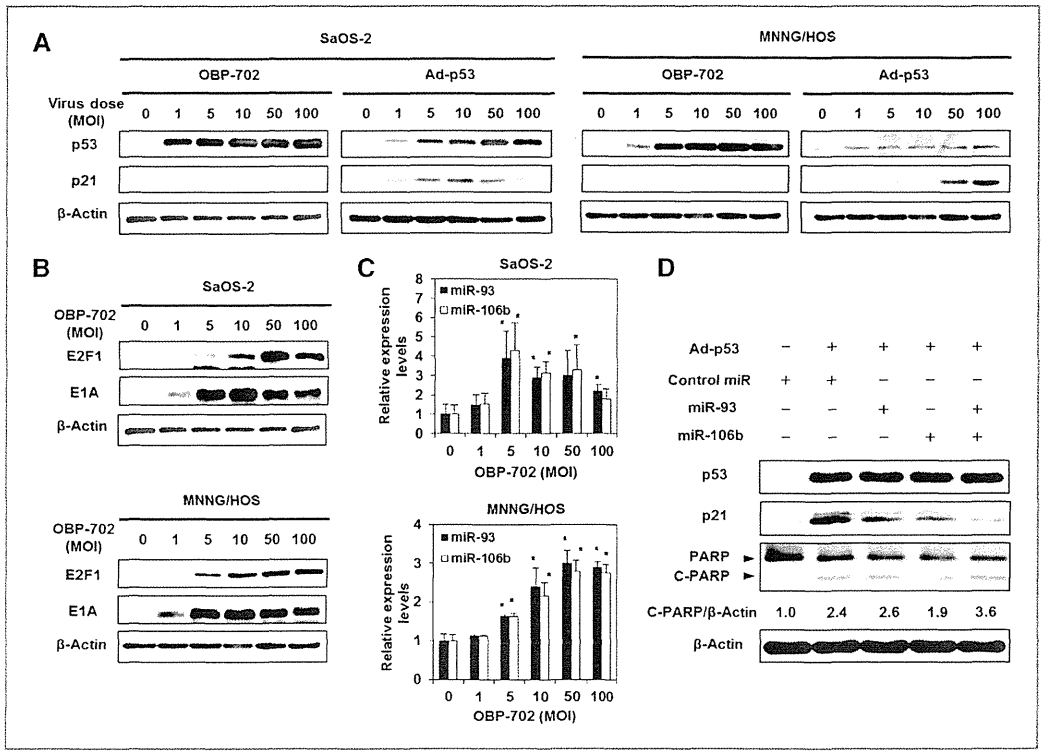

Figure 3. OBP-702 induces p53 overexpression with E1A-mediated p21 suppression via *miR-93* and *miR-106b* activation. A, expression of the p53 and p21 proteins in SaOS-2 and MNNG/HOS cells infected with OBP-702 or Ad-p53 at the indicated MOIs for 72 hours was assessed using Western blot analysis. B, expression of the E2F1 and viral E1A proteins in SaOS-2 and MNNG/HOS cells infected with OBP-702 at the indicated MOIs for 72 hours was assessed using Western blot analysis. C, expression of *miR-93* and *miR-106b* was assayed using qRT-PCR in SaOS-2 cells infected with OBP-702 at the indicated MOIs for 72 hours on 3 independent experiments. The values of *miR-93* and *miR-106b* at 0 MOI were set at 1, and the relative levels of *miR-93* and *miR-106b* at the indicated MOIs were plotted as fold induction. Bars, SD. Statistical significance was determined by Student *t* test. *, $P < 0.05$. D, SaOS-2 cells were transfected with 10 nmol/L *miR-93*, *miR-106*, or control miRNA 24 hours before Ad-p53 infection at an MOI of 100. At 48 hours after Ad-p53 infection, the expression levels of p53, p21, PARP, and C-PARP were examined by Western blot analysis. β-Actin was assayed as a loading control. By using ImageJ software, the expression level of C-PARP protein was calculated relative to its expression in the control miR–treated cells, whose expression level was designated as 1.0.

tumors (Fig. 5C). On histopathologic analysis, there were large necrotic areas in OBP-702–treated tumors but not in OBP-301- or Ad-p53–treated tumors (Fig. 5D). Moreover, the expression of the cell proliferation marker, Ki67, was also decreased, especially in OBP-702–treated tumor cells (Supplementary Fig. S6). These results suggest that OBP-702 eliminates tumor tissues more efficiently when compared with OBP-301 or Ad-p53.

Discussion

We previously reported that telomerase-specific replication-competent oncolytic adenovirus OBP-301 has strong antitumor activity in a variety of human epithelial and nonepithelial malignant cells (12, 14, 27). However, some human osteosarcoma cells were resistant to the cytopathic activity of OBP-301 (14). In this study, we showed that a novel p53-expressing oncolytic adenovirus, OBP-702, had increased *in vitro* and *in vivo* antitumor effects than did OBP-301 in human osteosarcoma cells (Fig. 1 and 5). OBP-702 induced increased apoptosis in association with p53 upregulation and p21 downregulation when compared with replication-deficient Ad-p53 (Fig. 2 and 3A). E1A-dependent upregulation of *miR-93* and *miR-106b* was involved in OBP-702–mediated suppression of p21 expression (Fig. 3). Moreover, p53-mediated DRAM activation with p21 suppression enhanced oncolytic adenovirus-mediated autophagy induction (Fig. 4). Recent studies suggest that transgene-expressing armed oncolytic adenoviruses are a promising antitumor strategy for induction of oncolytic and transgene-induced cell death (33). Although p53 overexpression has been shown to enhance antitumor

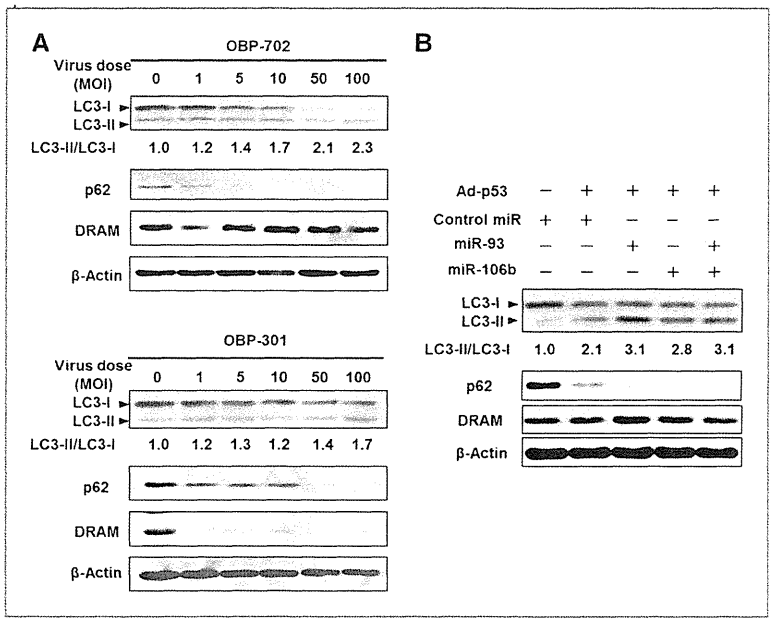

Figure 4. OBP-702 induces increased autophagy when compared with OBP-301. A, MNNG/HOS cells were infected with OBP-702 or OBP-301 at the indicated MOIs for 72 hours. Cell lysates were subjected to Western blot analysis for LC3, p62, and DRAM. B, SaOS-2 cells were transfected with 10 nmol/L *miR-93*, *miR-106*, or control miRNA 24 hours before Ad-p53 infection. At 48 hours after Ad-p53 infection at an MOI of 100, the expression levels of LC3, p62, and DRAM were examined by Western blot analysis. β-Actin was assayed as a loading control. By using ImageJ software, the ratio of LC3-II/LC3-I expressions was calculated relative to its expression in the mock-infected cells, whose expression level was designated as 1.0.

activity of oncolytic adenoviruses (34), the molecular mechanisms by which p53 mediates enhancement of the antitumor effect remain unclear. Recently, we reported that OBP-702 induces profound apoptosis through p53-dependent BAX upregulation and E1A-dependent p21 and MDM2 downregulation in epithelial malignant cells (26). Thus, oncolytic adenovirus-mediated p53 overexpression likely induces dual apoptotic and autophagic cell death pathways through p53-dependent BAX/DRAM activation and E1A-dependent p21/MDM2 suppression with E2F1-inducible *miR-93/106b* upregulation (Fig. 6).

OBP-702 efficiently suppressed the cell viability of both OBP-301–sensitive and -resistant osteosarcoma cells (Fig. 1). We previously reported that OBP-301–resistant SaOS-2 cells have no *hTERT* mRNA expression (Table 1), suggesting that SaOS-2 cells maintain telomere length through alternative lengthening of telomeres (ALT). As *hTERT* gene promoter is used for tumor-specific replication of OBP-301, ALT-type human osteosarcoma cells such as SaOS-2 cells may be resistant to OBP-301. However, ALT-type SaOS-2 cells showed similar sensitivity to OBP-702 as well as non–ALT-type MNNG/HOS cells (Fig. 1 and Table 1). These results suggest that p53 overexpression overcomes resistance to OBP-301 in ALT-type SaOS-2 cells. As the replication rate of OBP-702 was almost similar that of OBP-301 in ALT-type SaOS-2 cells (Supplementary Fig. S2), p53-induced cell death pathway would suppress the cell viability of ALT-type human osteosarcoma cells.

OBP-702–mediated p53 overexpression induced 2 types of programmed cell deaths (i.e., apoptosis and autophagy), thereby contributing to the enhancement of the antitumor effect of OBP-301 in human osteosarcoma cells (Fig. 2 and 4). As p53 downstream target p21 functions as a suppressor of apoptosis and autophagy (17, 18), p21 suppression may be a critical factor to induce dual programmed cell death pathways in response p53 overexpression. Suppression of p21 expression by genetic deletion or artificial p21 target microRNA has been shown to enhance the Ad-p53–induced apoptosis (18, 35). Inactivation of p21 by adenoviral E1A has been shown to enhance apoptosis in chemotherapeutic drug-treated human colon cancer cells that overexpress p53 (36). Genetic deletion of p21 has been also shown to induce autophagy in mouse embryonic fibroblasts treated with C (2)-ceramide or γ-irradiation (17). In contrast, p21 overexpression inhibited the Ad-p53–mediated apoptosis induction (18). Thus, E1A-mediated p21 downregulation would enhance p53-induced apoptosis and autophagy in OBP-702–infected cells.

E1A-dependent E2F1 activation and subsequent upregulation of E2F1-inducible miRNAs efficiently suppressed p21 expression, leading to the enhancement of p53-induced apoptosis and autophagy, in OBP-702–infected osteosarcoma cells (Figs. 2–4). Recent studies suggest that the cross-talk between p53 and E2F1 play a role in the regulation of diverse cell fates (37). For example, co-expression of p53 and E2F1 contributes to induction of apoptosis (38, 39). We previously showed

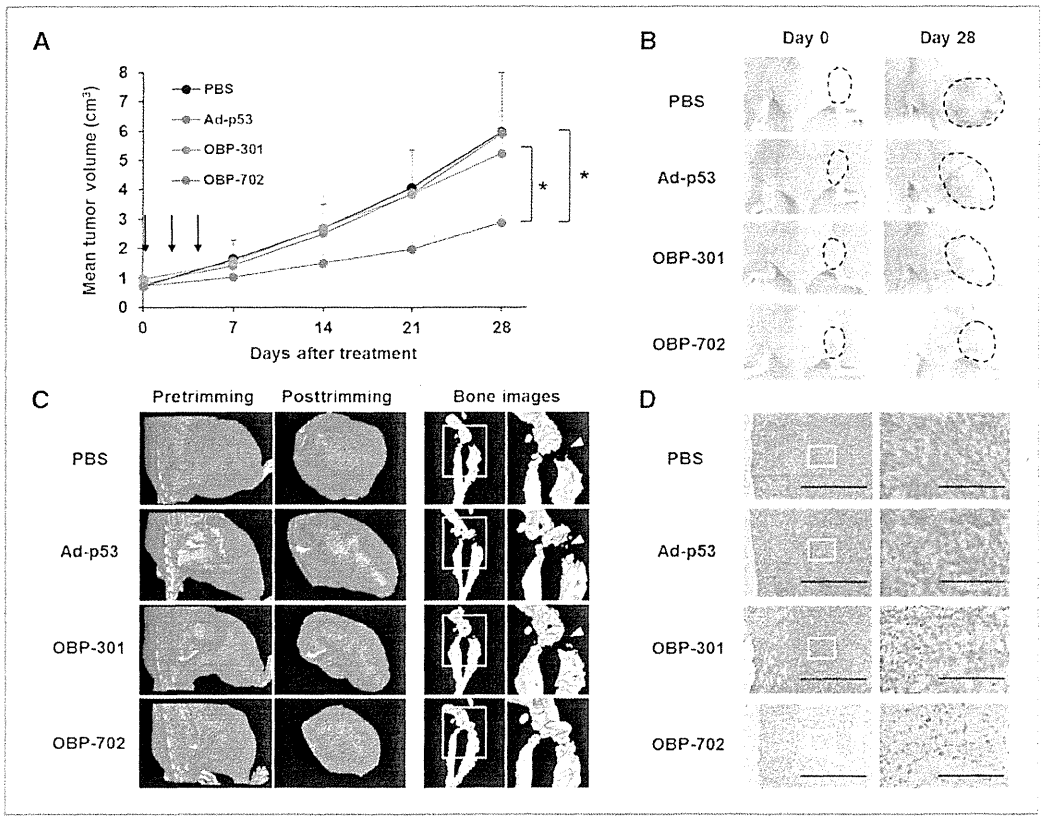

Figure 5. Antitumor effect of OBP-702 in an orthotopic MNNG/HOS osteosarcoma xenograft model. A, athymic nude mice were inoculated intratibially with MNNG/HOS cells (5×10^6 cells/site). Twenty-one days after inoculation (designated as day 0), Ad-p53, OBP-301, or OBP-702 were injected into the tumor with 1×10^8 PFUs on days 0, 2, and 4 (black arrows). PBS was used as a control. Three mice were used for each group. Each tumor volume was assessed by CT examination. Tumor growth was expressed as mean tumor volume ± SD. Statistical significance was determined by Student *t* test. *, $P < 0.05$. B, macroscopic appearance of MNNG/HOS tumors in nude mice on days 0 and 28 after treatment with PBS, Ad-p53, OBP-301, or OBP-702. Tumor masses are outlined by a dotted line. C, 3D-CT images of MNNG/HOS tumors. The tumor volumes were calculated by the image viewer (INTAGE Realia) based on 3D-CT images of tumors after trimming. The white arrowheads indicate the osteolytic areas within tumor tissues treated with PBS, Ad-p53, or OBP-301. Left side images are low magnification and right side images are high magnification of the area outlined by a white square. D, histologic analysis of the MNNG/HOS tumors. Tumor tissues were obtained on day 28 after first treatment with PBS, Ad-p53, OBP-301, or OBP-702. Paraffin-embedded sections of MNNG/HOS tumors were stained with hematoxylin and eosin solutions. There were large necrotic areas in MNNG/HOS tumors treated with OBP-702. Left side images are low magnification and right side images are high magnification of the area outlined by a white square. Left scale bars, 500 μm. Right scale bars, 100 μm.

that E2F1 enhanced Ad-p53–mediated apoptosis through p14ARF-dependent MDM2 downregulation (39) and that OBP-702 infection showed E1A-dependent MDM2 downregulation in association with apoptosis (26). Recently, E2F1 has been shown to suppress MDM2 expression by suppressing the promoter activity (40) or by inducing upregulation of *miR-25/32*, which targets MDM2 (41). Furthermore, E2F1-inducible *miR-93/106b* enhanced Ad-p53–induced apoptosis and autophagy via p21 suppression (Figs. 3D and 4B). Therefore, the cooperation between the MDM2/p53/p21 pathway and the E2F1/miRNA pathway may be involved in the induction of apoptotic and autophagic cell death in response to OBP-702.

OBP-702–mediated p53 overexpression enhanced autophagy that was induced by oncolytic adenovirus in human osteosarcoma cells. OBP-702 infection induced increased expression of DRAM and decreased expression of p62 when compared with OBP-301 (Fig. 4), suggesting that OBP-702–mediated p53 overexpression enhances autophagy through DRAM activation. We recently reported that OBP-301 induces autophagy through E1A-dependent activation of E2F1/*miR-7* pathway and subsequent suppression of EGF receptor

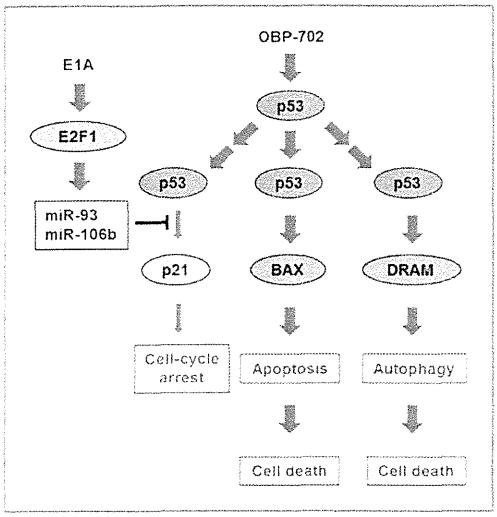

Figure 6. Outline of OBP-702–mediated induction of dual programmed cell death pathways. OBP-702 infection induces apoptosis and autophagy, leading to cell death, through p53-dependent BAX/DRAM upregulation and E1A-dependent p21 downregulation via E2F1-inducible *miR-93/106b* activation.

(EGFR; ref. 31). Restoration of p53 expression enhances the sensitivity to EGFR inhibitors in human cancer cells (42). Moreover, EGFR downregulation by transfection of specific antisense oligonucleotide promotes the differentiation status of human osteosarcoma U2OS cells (43). Thus, OBP-702 may induce differentiation as well as cell death through autophagy activation by DRAM upregulation and EGFR downregulation in human osteosarcoma cells.

The 3D-CT imaging system was a useful method to assess both tumor volume and bone destruction status in MNNG/HOS tumors. OBP-702–treated tumors were smaller and had less bone destruction than PBS-, Ad-p53-, or OBP-301–treated tumors (Fig. 5A and C). Recent reports have suggested that zoledronic acid suppresses tumor growth as well as osteolytic components in human osteosarcoma xenograft tumor models (44, 45). These results suggest that combination therapy with OBP-702 and zoledronic acid may be more effective and more protective against bone destruction in human osteosarcomas. Further study using a 3D-CT imaging system may provide important information about bone destruction status in osteosarcomas treated with OBP-702 and zoledronic acid.

Adenovirus-mediated *p53* gene therapy exerts an antitumor effect in human osteosarcoma cells (46). However, the antitumor activity of replication-deficient Ad-p53 is limited in some human osteosarcoma cells (47). Ad-p53–mediated p53 overexpression increases the sensitivity of human osteosarcoma cells to the chemotherapeutic drugs, cisplatin and doxorubicin (48). A synergistic antitumor effect between doxorubicin and roscovitine was also associated with autophagy induction in human osteosarcoma U2OS cells (49). As OBP-702 induced more profound apoptosis and autophagy than did OBP-301 or Ad-p53 (Fig. 2 and 4), combination therapy with OBP-702 and chemotherapeutic agents may be more effective than monotherapy with OBP-702. Moreover, a recent report has shown that p53-armed replication-competent oncolytic adenovirus is a safe antitumor agent in rodents and non-human primates (50). However, for clinical application of OBP-702, it must be necessary to establish the systemic delivery method and confirm the host biologic contributions in patients with cancer. Although there are some unsolved issues, the combination of p53-armed oncolytic adenovirus and chemotherapy may provide us a promising antitumor strategy against human osteosarcoma cells.

In conclusion, we clearly showed that the p53-expressing oncolytic adenovirus OBP-702 has a much stronger antitumor effect than does OBP-301. Oncolytic adenovirus-mediated *p53* gene transduction may induce dual apoptotic and autophagic cell death pathways through p53-dependent activation of cell death inducers and E1A-dependent suppression of cell death inhibitors, resulting in the enhancement of antitumor effect.

Disclosure of Potential Conflicts of Interest

Y. Urata is President & CEO of Oncolys BioPharma, Inc., the manufacturer of OBP-301 (Telomelysin). H. Tazawa and T. Fujiwara are consultants of Oncolys BioPharma, Inc. No potential conflicts of interest were disclosed by the other authors.

Authors' Contributions

Conception and design: J. Hasei, F. Uno, S. Kagawa, T. Ozaki, T. Fujiwara
Development of methodology: J. Hasei, F. Uno, S. Kagawa
Acquisition of data (provided animals, acquired and managed patients, provided facilities, etc.): J. Hasei, H. Tazawa, S. Osaki, Y. Yamakawa, A. Yoshida, T. Onishi, T. Ozaki
Analysis and interpretation of data (e.g., statistical analysis, biostatistics, computational analysis): J. Hasei, H. Tazawa, T. Fujiwara
Writing, review, and/or revision of the manuscript: J. Hasei, H. Tazawa, T. Kunisada, Y. Urata, T. Fujiwara
Administrative, technical, or material support (i.e., reporting or organizing data, constructing databases): H. Tazawa, T. Kunisada, Y. Hashimoto, S. Kagawa, Y. Urata, T. Ozaki
Study supervision: T. Sasaki, T. Kunisada, F. Uno, Y. Urata, T. Fujiwara

Acknowledgments

The authors thank Dr. Satoru Kyo (Kanazawa University) for providing the HOS and SaOS-2 cells and Tomoko Sueishi for her excellent technical support.

Grant Support

This study was supported by grants-in-aid from the Ministry of Education, Science, and Culture, Japan (T. Fujiwara) and grants from the Ministry of Health and Welfare, Japan (T. Fujiwara), and in part by the National Cancer Center Research and Development Fund (23-A-10) (T. Ozaki).

The costs of publication of this article were defrayed in part by the payment of page charges. This article must therefore be hereby marked *advertisement* in accordance with 18 U.S.C. Section 1734 solely to indicate this fact.

Received August 30, 2012; revised December 27, 2012; accepted December 29, 2012; published OnlineFirst January 11, 2013.

References

1. Ottaviani G, Jaffe N. The etiology of osteosarcoma. Cancer Treat Res 2009;152:15–32.
2. Damron TA, Ward WG, Stewart A. Osteosarcoma, chondrosarcoma, and Ewing's sarcoma: National Cancer Data Base Report. Clin Orthop Relat Res 2007;459:40–7.
3. Lewis IJ, Nooij MA, Whelan J, Sydes MR, Grimer R, Hogendoorn PC, et al. Improvement in histologic response but not survival in osteosarcoma patients treated with intensified chemotherapy: a randomized phase III trial of the European Osteosarcoma Intergroup. J Natl Cancer Inst 2007;99:112–28.
4. Bacci G, Longhi A, Versari M, Mercuri M, Briccoli A, Picci P. Prognostic factors for osteosarcoma of the extremity treated with neoadjuvant chemotherapy: 15-year experience in 789 patients treated at a single institution. Cancer 2006;106:1154–61.
5. Bielack SS, Kempf-Bielack B, Delling G, Exner GU, Flege S, Helmke K, et al. Prognostic factors in high-grade osteosarcoma of the extremities or trunk: an analysis of 1,702 patients treated on neoadjuvant cooperative osteosarcoma study group protocols. J Clin Oncol 2002; 20:776–90.
6. Siegel R, Naishadham D, Jemal A. Cancer statistics, 2012. CA Cancer J Clin 2012;62:10–29.
7. Buseman CM, Wright WE, Shay JW. Is telomerase a viable target in cancer? Mutat Res 2012;730:90–7.
8. Artandi SE, DePinho RA. Telomeres and telomerase in cancer. Carcinogenesis 2010;31:9–18.
9. Umehara N, Ozaki T, Sugihara S, Kunisada T, Morimoto Y, Kawai A, et al. Influence of telomerase activity on bone and soft tissue tumors. J Cancer Res Clin Oncol 2004;130:411–6.
10. Aogi K, Woodman A, Urquidi V, Mangham DC, Tarin D, Goodison S. Telomerase activity in soft-tissue and bone sarcomas. Clin Cancer Res 2000;6:4776–81.
11. Nakayama J, Tahara H, Tahara E, Saito M, Ito K, Nakamura H, et al. Telomerase activation by hTRT in human normal fibroblasts and hepatocellular carcinomas. Nat Genet 1998;18:65–8.
12. Kawashima T, Kagawa S, Kobayashi N, Shirakiya Y, Umeoka T, Teraishi F, et al. Telomerase-specific replication-selective virotherapy for human cancer. Clin Cancer Res 2004;10:285–92.
13. Nemunaitis J, Tong AW, Nemunaitis M, Senzer N, Phadke AP, Bedell C, et al. A phase I study of telomerase-specific replication competent oncolytic adenovirus (telomelysin) for various solid tumors. Mol Ther 2010;18:429–34.
14. Sasaki T, Tazawa H, Hasei J, Kunisada T, Yoshida A, Hashimoto Y, et al. Preclinical evaluation of telomerase-specific oncolytic virotherapy for human bone and soft tissue sarcomas. Clin Cancer Res 2011;17:1828–38.
15. Li G, Kawashima H, Ogose A, Ariizumi T, Xu Y, Hotta T, et al. Efficient virotherapy for osteosarcoma by telomerase-specific oncolytic adenovirus. J Cancer Res Clin Oncol 2011;137:1037–51.
16. Vousden KH, Prives C. Blinded by the light: the growing complexity of p53. Cell 2009;137:413–31.
17. Fujiwara K, Daido S, Yamamoto A, Kobayashi R, Yokoyama T, Aoki H, et al. Pivotal role of the cyclin-dependent kinase inhibitor p21WAF1/CIP1 in apoptosis and autophagy. J Biol Chem 2008;283:388–97.
18. Gorospe M, Cirielli C, Wang X, Seth P, Capogrossi MC, Holbrook NJ. p21(Waf1/Cip1) protects against p53-mediated apoptosis of human melanoma cells. Oncogene 1997;14:929–35.
19. Blagosklonny MV, el-Deiry WS. In vitro evaluation of a p53-expressing adenovirus as an anti-cancer drug. Int J Cancer 1996;67:386–92.
20. Zeng Y, Prabhu N, Meng R, Eldeiry W. Adenovirus-mediated p53 gene therapy in nasopharyngeal cancer. Int J Oncol 1997;11:221–6.
21. Clayman GL, el-Naggar AK, Lippman SM, Henderson YC, Frederick M, Merritt JA, et al. Adenovirus-mediated p53 gene transfer in patients with advanced recurrent head and neck squamous cell carcinoma. J Clin Oncol 1998;16:2221–32.
22. Swisher SG, Roth JA, Nemunaitis J, Lawrence DD, Kemp BL, Carrasco CH, et al. Adenovirus-mediated p53 gene transfer in advanced non-small-cell lung cancer. J Natl Cancer Inst 1999;91:763–71.
23. Shimada H, Matsubara H, Shiratori T, Shimizu T, Miyazaki S, Okazumi S, et al. Phase I/II adenoviral p53 gene therapy for chemoradiation resistant advanced esophageal squamous cell carcinoma. Cancer Sci 2006;97:554–61.
24. Fujiwara T, Tanaka N, Kanazawa S, Ohtani S, Saijo Y, Nukiwa T, et al. Multicenter phase I study of repeated intratumoral delivery of adenoviral p53 in patients with advanced non-small-cell lung cancer. J Clin Oncol 2006;24:1689–99.
25. Sakai R, Kagawa S, Yamasaki Y, Kojima T, Uno F, Hashimoto Y, et al. Preclinical evaluation of differentially targeting dual virotherapy for human solid cancer. Mol Cancer Ther 2010;9:1884–93.
26. Yamasaki Y, Tazawa H, Hashimoto Y, Kojima T, Kuroda S, Yano S, et al. A novel apoptotic mechanism of genetically engineered adenovirus-mediated tumour-specific p53 overexpression through E1A-dependent p21 and MDM2 suppression. Eur J Cancer 2012;48: 2282–91.
27. Hashimoto Y, Watanabe Y, Shirakiya Y, Uno F, Kagawa S, Kawamura H, et al. Establishment of biological and pharmacokinetic assays of telomerase-specific replication-selective adenovirus. Cancer Sci 2008;99:385–90.
28. Bagchi S, Raychaudhuri P, Nevins JR. Adenovirus E1A proteins can dissociate heteromeric complexes involving the E2F transcription factor: a novel mechanism for E1A trans-activation. Cell 1990;62: 659–69.
29. Emmrich S, Putzer BM. Checks and balances: E2F-microRNA crosstalk in cancer control. Cell Cycle 2010;9:2555–67.
30. Petrocca F, Vecchione A, Croce CM. Emerging role of miR-106b-25/miR-17-92 clusters in the control of transforming growth factor beta signaling. Cancer Res 2008;68:8191–4.
31. Tazawa H, Yano S, Yoshida R, Yamasaki Y, Sasaki T, Hashimoto Y, et al. Genetically engineered oncolytic adenovirus induces autophagic cell death through an E2F1-microRNA-7-epidermal growth factor receptor axis. Int J Cancer 2012;131:2939–50.
32. Crighton D, Wilkinson S, O'Prey J, Syed N, Smith P, Harrison PR, et al. DRAM, a p53-induced modulator of autophagy, is critical for apoptosis. Cell 2006;126:121–34.
33. Liu TC, Galanis E, Kirn D. Clinical trial results with oncolytic virotherapy: a century of promise, a decade of progress. Nat Clin Pract Oncol 2007;4:101–17.
34. van Beusechem VW, van den Doel PB, Grill J, Pinedo HM, Gerritsen WR. Conditionally replicative adenovirus expressing p53 exhibits enhanced oncolytic potency. Cancer Res 2002;62:6165–71.
35. Idogawa M, Sasaki Y, Suzuki H, Mita H, Imai K, Shinomura Y, et al. A single recombinant adenovirus expressing p53 and p21-targeting artificial microRNAs efficiently induces apoptosis in human cancer cells. Clin Cancer Res 2009;15:3725–32.
36. Chattopadhyay D, Ghosh MK, Mal A, Harter ML. Inactivation of p21 by E1A leads to the induction of apoptosis in DNA-damaged cells. J Virol 2001;75:9844–56.
37. Polager S, Ginsberg D. p53 and E2f: partners in life and death. Nat Rev Cancer 2009;9:738–48.
38. Wu X, Levine AJ. p53 and E2F-1 cooperate to mediate apoptosis. Proc Natl Acad Sci U S A 1994;91:3602–6.
39. Itoshima T, Fujiwara T, Waku T, Shao J, Kataoka M, Yarbrough WG, et al. Induction of apoptosis in human esophageal cancer cells by sequential transfer of the wild-type p53 and E2F-1 genes: involvement of p53 accumulation via ARF-mediated MDM2 down-regulation. Clin Cancer Res 2000;6:2851–9.
40. Tian X, Chen Y, Hu W, Wu M. E2F1 inhibits MDM2 expression in a p53-dependent manner. Cell Signal 2011;23:193–200.
41. Suh SS, Yoo JY, Nuovo GJ, Jeon YJ, Kim S, Lee TJ, et al. MicroRNAs/TP53 feedback circuitry in glioblastoma multiforme. Proc Natl Acad Sci U S A 2012;109:5316–21.
42. Huang S, Benavente S, Armstrong EA, Li C, Wheeler DL, Harari PM. p53 modulates acquired resistance to EGFR inhibitors and radiation. Cancer Res 2011;71:7071–9.
43. Salvatori L, Caporuscio F, Coroniti G, Starace G, Frati L, Russo MA, et al. Down-regulation of epidermal growth factor receptor induced by estrogens and phytoestrogens promotes the differentiation of U2OS human osteosarcoma cells. J Cell Physiol 2009;220: 35–44.

44. Dass CR, Choong PF. Zoledronic acid inhibits osteosarcoma growth in an orthotopic model. Mol Cancer Ther 2007;6:3263–70.
45. Labrinidis A, Hay S, Liapis V, Ponomarev V, Findlay DM, Evdokiou A. Zoledronic acid inhibits both the osteolytic and osteoblastic components of osteosarcoma lesions in a mouse model. Clin Cancer Res 2009;15:3451–61.
46. Temovoi VV, Curiel DT, Smith BF, Siegal GP. Adenovirus-mediated p53 tumor suppressor gene therapy of osteosarcoma. Lab Invest 2006;86:748–66.
47. Hellwinkel OJ, Muller J, Pollmann A, Kabisch H. Osteosarcoma cell lines display variable individual reactions on wildtype p53 and Rb tumour-suppressor transgenes. J Gene Med 2005;7:407–19.
48. Ganjavi H, Gee M, Narendran A, Parkinson N, Krishnamoorthy M, Freedman MH, et al. Adenovirus-mediated p53 gene therapy in osteosarcoma cell lines: sensitization to cisplatin and doxorubicin. Cancer Gene Ther 2006;13:415–9.
49. Lambert LA, Qiao N, Hunt KK, Lambert DH, Mills GB, Meijer L, et al. Autophagy: a novel mechanism of synergistic cytotoxicity between doxorubicin and roscovitine in a sarcoma model. Cancer Res 2008;68:7966–74.
50. Su C, Cao H, Tan S, Huang Y, Jia X, Jiang L, et al. Toxicology profiles of a novel p53-armed replication-competent oncolytic adenovirus in rodents, felids, and nonhuman primates. Toxicol Sci 2008;106: 242–50.

Published OnlineFirst September 30, 2013; DOI: 10.1158/1078-0432.CCR-13-0742

Cancer Therapy: Preclinical

Clinical Cancer Research

A Genetically Engineered Oncolytic Adenovirus Decoys and Lethally Traps Quiescent Cancer Stem-like Cells in S/G_2/M Phases

Shuya Yano[1], Hiroshi Tazawa[2], Yuuri Hashimoto[1], Yasuhiro Shirakawa[1], Shinji Kuroda[1], Masahiko Nishizaki[1], Hiroyuki Kishimoto[1], Futoshi Uno[1], Takeshi Nagasaka[1], Yasuo Urata[3], Shunsuke Kagawa[1], Robert M. Hoffman[4,5], and Toshiyoshi Fujiwara[1]

Abstract

Purpose: Because chemoradiotherapy selectively targets proliferating cancer cells, quiescent cancer stem-like cells are resistant. Mobilization of the cell cycle in quiescent leukemia stem cells sensitizes them to cell death signals. However, it is unclear that mobilization of the cell cycle can eliminate quiescent cancer stem-like cells in solid cancers. Thus, we explored the use of a genetically-engineered telomerase-specific oncolytic adenovirus, OBP-301, to mobilize the cell cycle and kill quiescent cancer stem-like cells.

Experimental Design: We established $CD133^+$ cancer stem-like cells from human gastric cancer MKN45 and MKN7 cells. We investigated the efficacy of OBP-301 against quiescent cancer stem-like cells. We visualized the treatment dynamics of OBP-301 killing of quiescent cancer stem-like cells in dormant tumor spheres and xenografts using a fluorescent ubiquitination cell-cycle indicator (FUCCI).

Results: $CD133^+$ gastric cancer cells had stemness properties. OBP-301 efficiently killed $CD133^+$ cancer stem-like cells resistant to chemoradiotherapy. OBP-301 induced cell-cycle mobilization from G_0–G_1 to S/G_2/M phases and subsequent cell death in quiescent $CD133^+$ cancer stem-like cells by mobilizing cell-cycle–related proteins. FUCCI enabled visualization of quiescent $CD133^+$ cancer stem-like cells and proliferating $CD133^-$ non-cancer stem-like cells. Three-dimensional visualization of the cell-cycle behavior in tumor spheres showed that $CD133^+$ cancer stem-like cells maintained stemness by remaining in G_0–G_1 phase. We showed that OBP-301 mobilized quiescent cancer stem-like cells in tumor spheres and xenografts into S/G_2/M phases where they lost viability and cancer stem-like cell properties and became chemosensitive.

Conclusion: Oncolytic adenoviral infection is an effective mechanism of cancer cell killing in solid cancer and can be a new therapeutic paradigm to eliminate quiescent cancer stem-like cells. *Clin Cancer Res; 19(23); 6495–505. ©2013 AACR.*

Introduction

Current cytotoxic chemoradiotherapy selectively targets proliferating cancer cells. Quiescent or dormant cancer cells in contrast are often drug-resistant and are a major impediment to cancer therapy (1, 2). Cancer stem-like cells or tumor-initiating cells (3–5) maintain a quiescent or dormant state, which appears to contribute to their resistance to conventional therapies (6–8). Recently, several therapeutic strategies have targeted inhibition of the cancer stem-like cell quiescent state. For example, treatment with arsenic trioxide enhanced the sensitivity of leukemia stem cells (LSC) to cytosine arabinoside through inhibition of LCS quiescence (9). Acute myeloid leukemia stem cells can be induced to enter the cell cycle and apoptosis by treatment with granulocyte colony-stimulating factor (10). However, it is still unclear whether cancer stem-like cells in solid tumors can also be eliminated by inducing them to cycle.

Viruses can infect target cells, multiply, cause cell death, and release viral particles. These features enable the use of viruses as anticancer agents that induce specific tumor lysis (11, 12). Adenoviral E1A, in particular, has been shown to exert tumor-suppressive functions, including enhancement of chemoradiotherapy-induced apoptosis via inhibition of the cellular DNA repair machinery (13)

Authors' Affiliations: [1]Department of Gastroenterological Surgery, Okayama University Graduate School of Medicine, Dentistry and Pharmaceutical Sciences; [2]Center for innovative clinical medicine, Okayama University Hospital, Okayama; [3]Oncolys BioPharma, Inc., Tokyo, Japan; [4]Department of Surgery, University of California San Diego; and [5]AntiCancer, Inc., San Diego, California

Note: Supplementary data for this article are available at Clinical Cancer Research Online (http://clincancerres.aacrjournals.org/).

Corresponding Author: Toshiyoshi Fujiwara, Department of Gastroenterological Surgery, Okayama University Graduate School of Medicine, Dentistry, and Pharmaceutical Sciences, 2-5-1 Shikata-cho, Kita-ku, Okayama 700-8558, Japan. Phone: 81-86-235-7255; Fax: 81-86-221-8775; E-mail: toshi_f@md.okayama-u.ac.jp

doi: 10.1158/1078-0432.CCR-13-0742

Published OnlineFirst September 30, 2013; DOI: 10.1158/1078-0432.CCR-13-0742

Translational Relevance

Current chemotherapy and radiotherapy target proliferating cancer cells, while having little effect on dormant cancer cells. Cancer stem–like cells can maintain a quiescent or dormant state, which contributes largely to their resistance to conventional therapies. Recently, several therapeutic strategies have targeted inhibition of the quiescent state in leukemia stem cells. However, it is still unclear whether cancer stem–like cells in solid tumors can also be eliminated by inhibition of their dormant state. Here, we show that a telomerase-specific adenovirus, OBP-301, mobilizes quiescent cancer stem–like cells to cycle and lethally traps them into S-phase. Moreover, we showed by spatiotemporal treatment dynamics that OBP-301 decoyed quiescent cancer stem–like cells in tumor spheres and xenografts into an S-phase trap where they lost viability and cancer stem–like cell properties and become chemosensitive. Thus, our data demonstrated that cell-cycle mobilization and S/G_2/M phase trapping induced by adenoviral infection is an effective mechanism of killing cancer stem–like cells in solid cancers.

and inhibition of cell proliferation via suppression of EGH receptor (EGFR; ref. 14) and HER-2 (15). It has been recently reported that an oncolytic adenovirus efficiently eradicates cancer stem–like cells as well as non–cancer stem–like cells in brain tumors, breast cancer, and esophageal cancer (16–18).

In the present study, we isolated CD133$^+$ subpopulations from radioresistant cells in human gastric cancer cell lines and characterized them as cancer stem–like cells. By using multicolor cell-cycle imaging that color codes the quiescent cancer stem–like cells and proliferating non–cancer stem–like cells, we showed by treatment dynamics that a genetically engineered telomerase-specific oncolytic adenovirus, OBP-301 (19, 20), eradicates dormant CD133$^+$ cancer stem–like cells via cell-cycle mobilization both in tumor spheres and in subcutaneous tumors.

Materials and Methods

Cell lines and radiation treatment

The human gastric cancer cell lines MKN45 and MKN7 were maintained according to the vendor's specifications (21). Radioresistant MKN45 and MKN7 cells were established by administration of radiation treatments using an X-ray generator (MBR-1505R; Hitachi Medical Co.).

Recombinant adenoviruses

The recombinant tumor-specific, replication-selective adenovirus vector OBP-301 (Telomelysin), in which the promoter element of the human telomerase reverse transcriptase (hTERT) gene drives the expression of E1A and E1B genes linked to an internal ribosome entry site, was previously constructed and characterized (19, 22).

Isolation of CD133$^+$ and CD133$^-$ cells by flow cytometry

After incubation with an anti-CD133/2(293C)-allophycocyanin antibody (Miltenyi Biotec), CD133$^+$ cells were sorted by flow cytometry using a FACSAria flow cytometer (Becton Dickinson). CD133$^+$ and CD133$^-$ cells were separated by flow cytometry just before each experiment to ensure that the purity of the CD133$^+$ population was greater than 70%, and the purity of CD133$^-$ cells was above 99%.

Cell viability assay

CD133$^+$ and CD133$^-$ cells (5×10^2 cells/well) in 96-well plates were treated with OBP-301, cisplatin, or radiation at the indicated doses. Cell viability was determined on day 5 after treatment using the Cell Proliferation Kit II (Roche Molecular) according to the manufacturer's protocol.

Establishment of MKN45 cells stably transfected with FUCCI vector plasmids

FUCCI (fluorescent ubiquitination-based cell-cycle indicator) (23) was used to visualize the cell-cycle phases. Plasmids, expressing mKO2-hCdt1 (GFP) or mAG-hGem (orange fluorescence protein), were obtained from the Medical & Biological Laboratory. Plasmids expressing mKO2-hCdt1 or mAG-hGem were transfected into radioresistant MKN45 cells using Lipofectamine LTX (Invitrogen).

Western blot analysis

The primary antibodies used were: mouse anti-CD133/1(W6B3C) monoclonal antibody (mAb; Miltenyi Biotec); rabbit anti-E2F1 polyclonal antibody (pAb) (Santa Cruz Biotechnology); mouse anti-Ad5 E1A mAb (BD Pharmingen); mouse anti-c-Myc pAb, rabbit anti-phospho-Akt mAb, rabbit anti-Akt mAb, mouse anti-p27 mAb (all from Cell Signaling Technology); mouse anti-p53 mAb, mouse anti-p21 mAb (both from CALBIOCHEM Merck4 Biosciences); and mouse anti-β-actin mAb (Sigma-Aldrich). Immunoreactive bands on the blots were visualized using enhanced chemiluminescence substrates (ECL Plus; GE Healthcare).

Subcutaneous MKN45 tumor xenograft model

To evaluate a tumorigenicity of CD133$^+$ and CD133$^-$ cells, purified CD133$^+$ and CD133$^-$ cells from radioresistant MKN45 were inoculated at a density of 1×10^5 cells/site on the right and left sides, respectively, of the flank of 5-week-old female NOD/SCID mice (Charles River Laboratories) or athymic nude mice (Charles River Laboratories). To evaluate the *in vivo* antitumor efficacy of OBP-301, cisplatin, or radiation, the radioresistant MKN45 cells were inoculated at a density of 5×10^6 cells/site into the flank of 5-week-old female athymic nude mice. OBP-301 [1×10^8 plaque-forming units (PFU)] was injected into the tumors. Cisplatin (4 mg/kg body weight) was intraperitoneally injected and ionizing radiation (2 Gy) was administered to tumors after protection of normal tissues. Mice were treated every 3 days for a total of three treatments.

Published OnlineFirst September 30, 2013; DOI: 10.1158/1078-0432.CCR-13-0742

Imaging of MKN45 cells expressing cell-cycle–dependent fluorescent proteins

Time lapse images of FUCCI-expressing CD133$^+$ and CD133$^-$ radioresistant MKN45 cells were acquired using a confocal laser scanning microscope (FV10i; Olympus). Cross-sections of FUCCI-expressing tumors were imaged using a confocal laser scanning microscope (FV-1000; Olympus).

Treatment of subcutaneous FUCCI-expressing MKN45 tumors

To evaluate the *in vivo* antitumor efficacy of OBP-301, cisplatin, paclitaxel, or their combination, the FUCCI-expressing MKN45 cells were inoculated at a density of 5×10^6 cells/site into the flank of 5-week-old female athymic nude mice (Charles River Laboratories). OBP-301 (1×10^8 PFU/tumor) was injected into the tumors. Cisplatin (4 mg/kg) and paclitaxel (5 mg/kg) were injected intraperitoneally. Mice were treated every 3 days for a total of 3 to 5 treatments.

Statistical analysis

Data are shown as means ± SD. For comparison between 2 groups, significant differences were determined using the Student *t* test. For comparison of more than 2 groups, statistical significance was determined with a one-way ANOVA followed by a Bonferroni multiple-group comparison test. $P < 0.05$ was considered significant.

Results

CD133$^+$ cells in human gastric cancer cells are cancer stem–like

Cancer stem–like cells are more resistant to radiotherapy than non–cancer stem–like cells (24–26). To enrich cancer stem–like subpopulations, we established radioresistant MKN45 and MKN7 human gastric cancer cells. Radioresistant MKN45 and MKN7 cells had a significantly higher percentage of CD133$^+$ cells than parental cells (Fig. 1A and Supplementary Fig. S1A). We hypothesized that CD133 in gastric cancer would identify cancer cells with stem-like properties, such as asymmetric cell division, *in vitro* proliferation, dormancy, sphere formation, and *in vivo* tumorigenicity (5, 6). To investigate the asymmetric division of CD133$^-$ cells, we determined whether CD133$^+$ cells produce both CD133$^+$ and CD133$^-$ cells. CD133$^+$ cells generated both CD133$^+$ and CD133$^-$ cells, whereas CD133$^-$ cells could not produce CD133$^+$ cells (Supplementary Fig. S2). We compared *in vitro* proliferation of CD133$^+$ and CD133$^-$ cells. CD133$^+$ cells produced larger colonies than CD133$^-$ cells (Fig. 1B and Supplementary Fig. S3). CD133$^+$ cells made significantly much more tumor spheres than CD133$^-$ cells (Fig. 1B). CD133$^+$ cells produced tumors in immunodeficient nude mice and NOD/SCID mice, whereas CD133$^-$ cells did not generate tumors in either nude on NOD/SCID mice (Supplementary Fig. S4 and Fig. 1B). Furthermore, CD133$^+$ cells in radioresistant MKN45 and MKN7 cells were significantly more resistant to 5-fluorouracil, cisplatin, paclitaxel, and radiation than CD133$^-$ cells (Fig. 1C and Supplementary Fig. S1B). These data indicate that CD133$^+$ cells are cancer stem–like.

Quiescent CD133$^+$ cancer stem–like cells and cycling CD133$^-$ non–cancer stem–like cells are independently visualized by fluorescent cell-cycle indicator technology

Sakaue-Sawano and colleagues have reported that the cell-cycle state in viable cells can be visualized using the FUCCI system (23). We established FUCCI-expressing CD133$^+$ or CD133$^-$ radioresistant MKN45 cells, in which cell nuclei in G_0–G_1, S, or G_2–M phases exhibit red, yellow, or green fluorescence, respectively. We compared the cell-cycle phase of FUCCI-expressing CD133$^+$ or CD133$^-$ cells. Time-lapse imaging showed that most of CD133$^+$ cells were quiescent in G_0–G_1 phase with red fluorescent nuclei compared with CD133$^-$ cells (Fig. 1D). Similar results were also observed in flow cytometric analysis of the cell cycle (Supplementary Fig. S5A and S5B). CD133$^+$ cells had similar proliferation rates as CD133$^-$ cells until 3 days after seeding. CD133$^+$ cells showed lower proliferation rates than CD133$^-$ cells 5 days after seeding (Fig. 1D). This result was consistent with the cell-cycle status of CD133$^+$ cells which had an increased percentage of cells in G_0–G_1 phase. Moreover, we examined cell-cycle–related protein (27) expression in CD133$^+$ and CD133$^-$ cells. CD133$^+$ cells showed higher expressions of p53, p21, and p27 proteins compared with CD133$^-$ cells (Supplementary Fig. S8), suggesting that these proteins are involved in the maintenance of quiescent cancer stem–like cells.

OBP-301 efficiently kills cancer stem–like cells and reduces cancer stem–like cell frequency via enhanced viral replication

To evaluate the efficacy of OBP-301 against CD133$^+$ cancer stem–like cells, we treated CD133$^+$ and CD133$^-$ cells from radioresistant MKN45 and MKN7 cells with OBP-301. OBP-301 similarly killed CD133$^+$ and CD133$^-$ cells (Fig. 2A and Supplementary Fig. S1B). Next we investigated whether OBP-301 could decrease cancer stem–like cell frequency. Flow cytometric analysis showed that OBP-301 significantly decreased the percentage of CD133$^+$ cells compared with cisplatin or radiation (Fig. 2A). Expression of *CD133* mRNA was closely associated with the population of CD133$^+$ cells (Supplementary Fig. S6). OBP-301 significantly suppressed the expression of *CD133* mRNA compared with cisplatin and radiation (Supplementary Fig. S7). Western blot analysis also showed that cisplatin and radiation, but not OBP-301, increased CD133 expression 3- to 5-fold in CD133$^+$ cells (Fig. 2D). Moreover, pretreatment of CD133$^+$ cells with OBP-301, but not cisplatin or radiation, significantly decreased the number of tumor spheres (Supplementary Fig. S13). These data indicated that OBP-301 kills both CD133$^+$ and CD133$^-$ cells and reduces cancer stem–like cell frequency.

To further explore the efficacy of OBP-301 against CD133$^-$ cancer stem–like cells, we assessed the relationship between hTERT activity and viral replication. OBP-301 contains the hTERT promoter, which allows it to tumor-specifically regulate the gene expression of E1A and E1B for viral replication (19). Quantitative reverse transcription

Published OnlineFirst September 30, 2013; DOI: 10.1158/1078-0432.CCR-13-0742

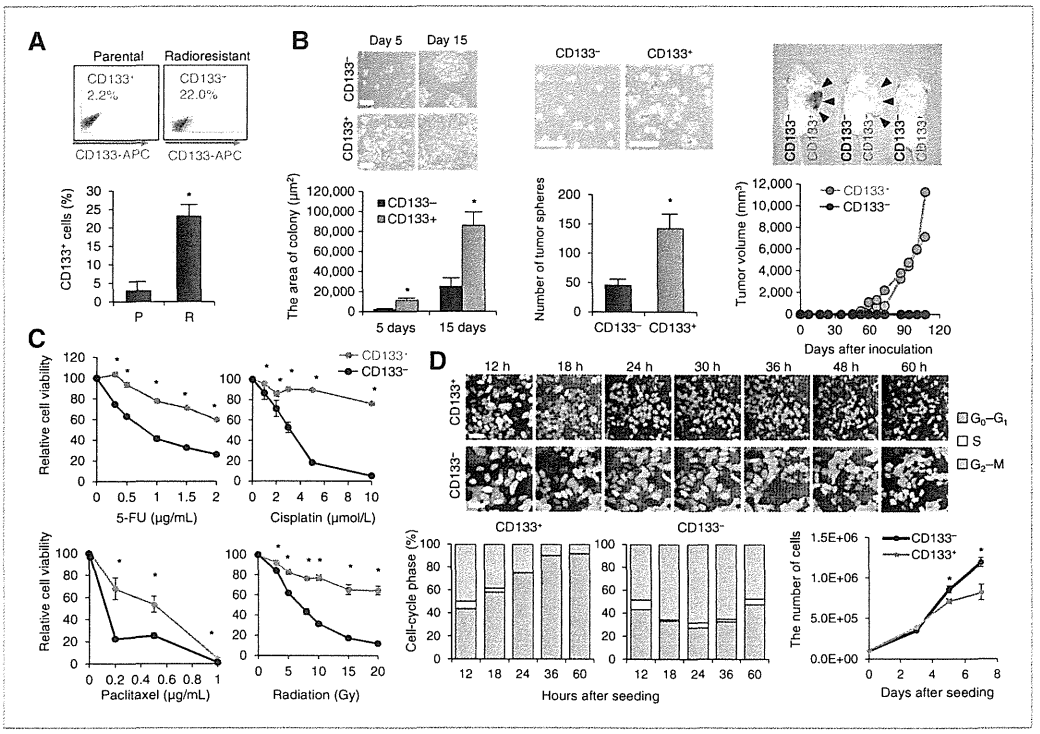

Figure 1. CD133$^+$ cancer stem–like cells in human gastric cancer exhibit cancer stem–like cell properties and are more quiescent. A, flow cytometric analysis of CD133 expression in parental (P) and radioresistant (R) MKN45 cells. Representative dot plots (top) and data from 5 experiments (bottom) are shown. B, CD133$^+$ MKN45 cancer cells exhibit cancer stem–like properties. Representative images of colonies from CD133$^+$ or CD133$^-$ cells. Histogram shows the size of colonies from CD133$^+$ or CD133$^-$ cells (left). Quantitative measurement of the tumor sphere–forming potential of CD133$^+$ and CD133$^-$ cells (middle). Representative images of tumor spheres derived from CD133$^+$ and CD133$^-$ cells. Histogram shows the numbers of tumor spheres from CD133$^+$ or CD133$^-$ cells. Scale bars, 500 μm. Tumorigenicity of CD133$^+$ and CD133$^-$ cells in immunodeficient NOD/SCID mice (right). Growth curve of each tumor and representative photographs are shown. C, sensitivity of CD133$^+$ and CD133$^-$ cells from radioresistant MKN45 cells to 5-fluorouracil, cisplatin, paclitaxel, and irradiation. D, time-lapse imaging of CD133$^+$ and CD133$^-$ cells from radioresistant MKN45 cells expressing cell-cycle–dependent fluorescent proteins (FUCCI; top). The cells in G_0–G_1, S, or G_2–M phases appear red, yellow, or green, respectively. Histogram shows the cell-cycle phase of FUCCI-expressing CD133$^+$ and CD133$^-$ cells cultured for 48 hours after sorting (bottom left). The percentage of cells in G_0–G_1, S, and G_2–M phases are shown. Cell proliferation rate of CD133$^+$ and CD133$^-$ cells (bottom right). Scale bars, 50 μm. Data are shown as means ± SD (n = 5). *, $P < 0.01$.

PCR (qRT-PCR) showed that CD133$^-$ cells had a significant, 3-fold higher expression of *hTERT* mRNA than CD133$^-$ cells (Fig. 2B), suggesting that CD133$^+$ cancer stem–like cells have a higher activity of hTERT than CD133$^-$ cells. Next we compared the expression of *E1A* mRNA and E1A protein in CD133$^+$ cells and in CD133$^-$ cells. qRT-PCR showed that the expression of *E1A* mRNA in CD133$^+$ cells was higher than that in CD133$^-$ cells (Fig. 2B). Western blotting showed that the expression of E1A in CD133$^+$ cells was higher than that in CD133$^-$ cells (Fig. 2B). Furthermore, we compared the copy number of the E1A gene, which is indicative of viral replication, in CD133$^+$ and CD133$^-$ cells after infection with OBP-301. As expected, the copy number of the E1A gene in CD133$^+$ cells was significantly higher than that in CD133$^-$ cells (Fig. 2B). These data indicate that OBP-301 is efficiently cytopathic for CD133$^+$ cells due to enhanced viral replication.

OBP-301 mobilizes and lethally traps quiescent cancer stem–like cells into S-phase in monolayer culture

To examine whether OBP-301 could change the cell-cycle phase of quiescent CD133$^+$ cells, we treated FUCCI-expressing CD133$^+$ cells with OBP-301. Time-lapse imaging showed that OBP-301 infection significantly decreased the percentage of CD133$^+$ cells in G_0–G_1 phase, increased the percentage of CD133$^-$ cells in S-phase, and killed them in S-phase (Fig. 2C and Supplementary Movie S1). Similar results were also observed in flow cytometric analysis of the cell cycle (Supplementary Fig. S5C and S5D). These results suggest that OBP-301 induces cell-cycle activation of quiescent CD133$^-$ cells from G_0–G_1 phase to S-phase and kills them. We next assessed the molecular mechanism by which OBP-301 induces mobilization of the cell cycle in quiescent cancer stem–like cells. OBP-301 increased the expression of E2F1, c-Myc, and phospho-Akt proteins that function as

Published OnlineFirst September 30, 2013; DOI: 10.1158/1078-0432.CCR-13-0742

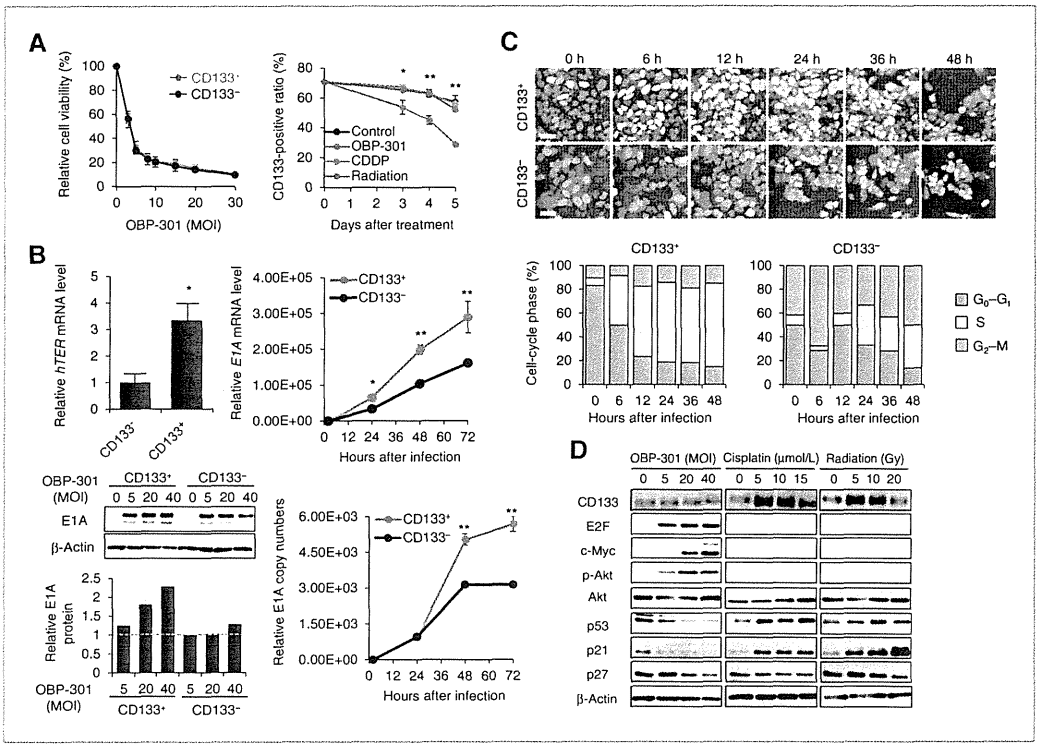

Figure 2. OBP-301 lethally induces S-phase transition of quiescent CD133$^-$ cancer stem–like cells and decreases cancer stem–like cell frequency via enhanced viral replication. A, OBP-301 efficiently kills CD133$^+$ cancer stem–like cells. Left, viability of CD133$^+$ and CD133$^-$ MKN45 cells after OBP-301 infection. Right, CD133-positive ratio of MKN45 cells treated with OBP-301, cisplatin, or radiation was analyzed by flow cytometry. B, OBP-301 can replicate more in CD133$^-$ cells that have more hTERT activity than in CD133$^-$ cells. Expression of *hTERT* mRNA in CD133$^-$ and CD133$^-$ MKN45 cells assessed by qRT-PCR (top left). The relative levels of *hTERT* mRNA were calculated after normalization with reference to the expression of *PBGD* mRNA. Expression of *E1A* mRNA in CD133$^+$ and CD133$^-$ MKN45 cells after OBP-301 infection at an MOI of 10 PFU/cell for 2 hours. Expression of *E1A* mRNA was analyzed over the following 3 days by qRT-PCR (top right). The relative levels of *E1A* mRNA were calculated after normalization with reference to the expression of *GAPDH* mRNA. Western blot analysis of E1A expression in CD133$^+$ and CD133$^-$ MKN45 cells treated with OBP-301 for 48 hours (bottom left). Quantitative relative expression level of E1A protein, normalized to β-actin, using NIH ImageJ software (bottom left). Quantitative measurement of viral DNA replication in CD133$^+$ and CD133$^-$ MKN45 cells after OBP-301 infection at an MOI of 10 PFU/cell for 2 hours (bottom right). *E1A* copy number was analyzed over the following 3 days using qPCR. C, time-lapse imaging of FUCCI-expressing CD133$^+$ and CD133$^-$ cells treated with OBP-301 at an MOI of 20 PFU/cell. The cells in G_0–G_1, S, or G_2–M phases appear red, yellow, or green, respectively. Histogram shows the cell-cycle phases of FUCCI-expressing CD133$^-$ and CD133$^-$ cells treated with OBP-301 for 48 hours. The percentage of cells in G_0–G_1, S, and G_2–M phases are shown. D, Western blot analysis of E2F1, c-Myc, phospho-Akt, Akt, p53, p21, and p27 expression in CD133$^+$ cells treated with OBP-301, cisplatin, or radiation for 48 hours. β-Actin was assayed as a loading control for all experiments. Data are shown as means ± SD ($n = 5$). *, $P < 0.05$; **, $P < 0.01$.

cell-cycle accelerators (27) and decreased the expression of p53, p21, and p27 proteins that function as cell-cycle brakes (27) in quiescent CD133$^+$ cells (Fig. 2D). In contrast, cisplatin and radiation increased the expression of p53 and p21 proteins (Fig. 2D). We further examined whether adenoviral E1A altered the expression of these proteins in CD133$^-$ cells. E1A-expressing OBP-301 and Ad5, but not E1A-defficient dl312, similarly altered the expression of these proteins in CD133$^-$ cells (Supplementary Fig. S9). These results indicate that OBP-301 induces cell-cycle progression through upregulation of E2F-related proteins and downregulation of p53-related and p27 proteins by enhanced adenoviral E1A in quiescent cancer stem–like cells.

Three-dimensional tumor spheres maintain a CD133$^-$ subpopulation by remaining quiescent

Formation of tumor spheres under serum-free conditions is frequently used to maintain cancer stem–like cell subpopulations (28). The addition of serum makes floating undifferentiated tumor spheres adherent and their cells differentiate into adherent cells (29). Therefore, we hypothesized that tumor spheres maintained their cancer stem–like cell frequency due to quiescence.

Published OnlineFirst September 30, 2013; DOI: 10.1158/1078-0432.CCR-13-0742

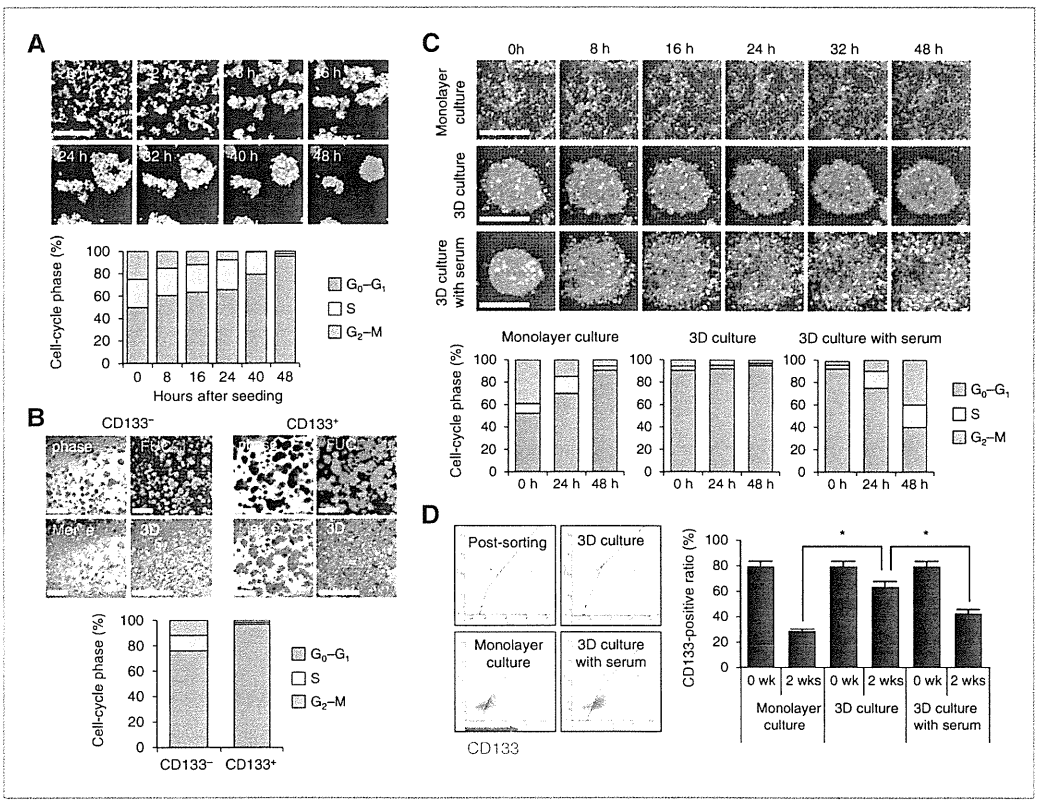

Figure 3. Three-dimensional tumor spheres maintain CD133$^+$ cells by the cell cycle arrest. A, time-lapse images of FUCCI-expressing CD133$^+$ cells in 3-dimensional culture without serum. Purified FUCCI-expressing CD133$^+$ cells were cultured on agar in serum-free medium containing EGF and bFGF for 48 hours (top). The cells in G_0–G_1, S, or G_2–M phases appear red, yellow, or green, respectively. Histogram shows the cell-cycle phase of FUCCI-expressing CD133$^+$ cells in 3-dimensional culture without serum (bottom). The percentage of cells in G_0–G_1, S, and G_2–M phases are shown. B, representative images of tumor spheres formed from FUCCI-expressing CD133$^+$ and CD133$^-$ cells (top). Histogram shows the cell-cycle phase of tumor spheres from FUCCI-expressing CD133$^+$ and CD133$^-$ cells (bottom). C, time-lapse images of FUCCI-expressing CD133$^+$ cells in monolayer culture or FUCCI-expressing tumor spheres in 3-dimensional culture without serum (3D without serum) or tumor spheres in monolayer culture with serum (monolayer culture; top). Histogram shows the cell-cycle phase of FUCCI-expressing CD133$^+$ cells in 2D culture, FUCCI-expressing established tumor spheres in 3D without serum, or tumor spheres on plastic culture with serum (monolayer culture; bottom). D, comparison of changes in the CD133$^+$-positive ratio in monolayer culture, tumor spheres in 3D culture without serum, or with serum. Representative dot plots (left) and data from 3 experiments (right) are shown. Data are shown as means ± SD (n = 5). *, $P < 0.01$. Scale bars, 500 μm.

CD133$^+$ cells aggregated and formed tumor spheres, and arrested in G_0–G_1 phase (Fig. 3A). Tumor spheres formed from CD133$^+$ cells contained more quiescent cells than those formed from CD133$^-$ cells (Fig. 3B). Moreover, established tumor spheres formed from CD133$^+$ cells remained quiescent in 3-dimensional culture without serum (Fig. 3C). In contrast, established tumor spheres, after addition of serum, exited from the quiescent state and began to cycle, divide, and increase (Fig. 3C and Supplementary Movie S2). Flow cytometric analysis showed that CD133$^-$ cells could be maintained in tumor spheres cultured in serum-free medium for 2 weeks, whereas the percentage of CD133$^+$ cells significantly decreased in monolayer cultures or in tumor spheres cultured in serum-containing medium (Fig. 3D). These data indicate that tumor spheres maintain their cancer stem-cell frequency by remaining dormant.

Real-time imaging spatiotemporally shows OBP-301 eliminates dormant tumor spheres by cell-cycle mobilization and S/G_2/M phase trapping

To further evaluate OBP-301-induced cell-cycle mobilization and S-phase trapping in dormant tumor spheres, we visualized the treatment dynamics of FUCCI-expressing tumor spheres infected with OBP-301. Time-lapse imaging showed that OBP-301 infected quiescent CD133$^+$ cells at the periphery of the spheres and then induced S and G_2–M

Published OnlineFirst September 30, 2013; DOI: 10.1158/1078-0432.CCR-13-0742

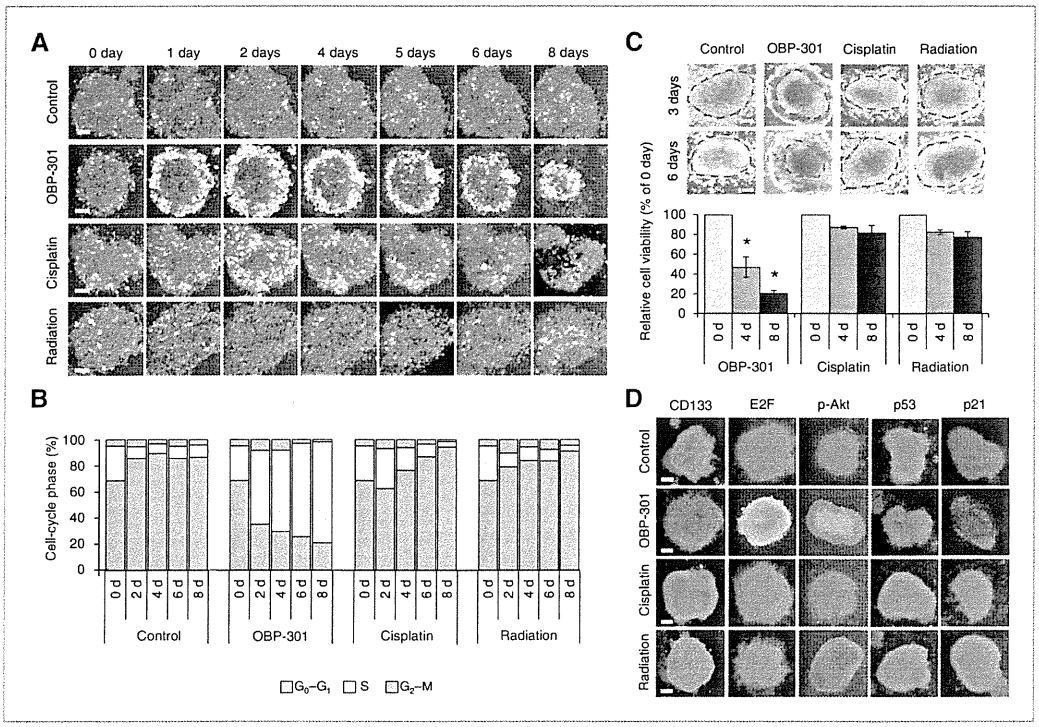

Figure 4. Visualization of elimination of dormant tumor spheres by virus infection. A, time-lapse images of tumor spheres treated with OBP-301 (5×10^6 PFU), cisplatin (10 μmol/L), or radiation (10 Gy). The cells in G_0–G_1, S, or G_2–M phases appear red, yellow, or green, respectively. B, histogram shows the cell-cycle phases of the spheres with OBP-301, cisplatin, or radiation. The percentage of cells in G_0–G_1, S, and G_2–M phases are shown. C, representative images of control, OBP-301-, cisplatin-, or radiation-treated spheres (top). Histogram shows the relative cell viability of treated tumor spheres (bottom). D, the $CD133^+$ tumor spheres treated as above were stained for E2F1, phospho-Akt, p53, and p21. Immuofluorescence staining was visualized by confocal laser microscopy. Scale bars, 100 μm. Data are shown as means ± SD ($n = 5$). *, $P < 0.01$.

phase entry, leading to cellular death by viral replication (Fig. 4A). Moreover, as OBP-301 penetrated into the deeper layers, tumor spheres gradually shrunk after virus infection (Fig. 4A and C). In contrast, cisplatin and radiation did not affect the cell-cycle phase or the size of tumor spheres (Figs. 4A–C and Supplementary Movie S3). Immunofluorescence staining of tumor spheres also confirmed that OBP-301 infection downregulated CD133, p53, and p21 expression and upregulated E2F1 and phospho-Akt expression in tumor spheres (Fig. 4D). These results suggest that OBP-301 efficiently eradicates dormant tumor spheres resistant to conventional therapies by mobilizing them into an $S/G_2/M$ phase trap.

OBP-301 efficiently kills dormant cancer stem–like cells in established human tumor xenografts by cell-cycle mobilization and $S/G_2/M$ phase trapping, thereby reducing cancer stem–like cell frequency

To further confirm whether OBP-301 efficiently reduced $CD133^+$ cancer stem–like cell frequency within tumor tissues (Supplementary Fig. S10A), we investigated the expression of *CD133* mRNA and the CD133-positive ratio in subcutaneous tumors derived from radioresistant MKN45 cells after treatment of OBP-301, cisplatin, or irradiation. Suppression of tumor growth by OBP-301 (Fig. 5A) was accompanied by a significant decrease in *CD133* mRNA at 2 weeks after the final treatment (Fig. 5B). In contrast, although cisplatin and radiation also suppressed tumor growth to a similar extent as OBP-301 (Fig. 5A), cisplatin did not affect, and radiation significantly increased *CD133* mRNA expression at 1 week after the final treatment (Fig. 5B). Immunohistochemistry of CD133-stained tumor sections also showed that OBP-301 reduced the frequency of $CD133^+$ cells, whereas cisplatin and irradiation increased the frequency compared with control (Fig. 5B).

Next, we visualized treatment dynamics in established FUCCI-expressing MKN45 tumor xenografts with or without OBP-301 infection (Supplementary Fig. S10B). FUCCI-expressing MKN45 tumors had a distribution of cancer cells in G_0–G_1, S, and G_2–M phases (Fig. 5A). As tumors grew bigger, cancer cells in G_0–G_1 phase increased (Fig. 5C and D), indicating the existence of dormant cancer cells.

Published OnlineFirst September 30, 2013; DOI: 10.1158/1078-0432.CCR-13-0742

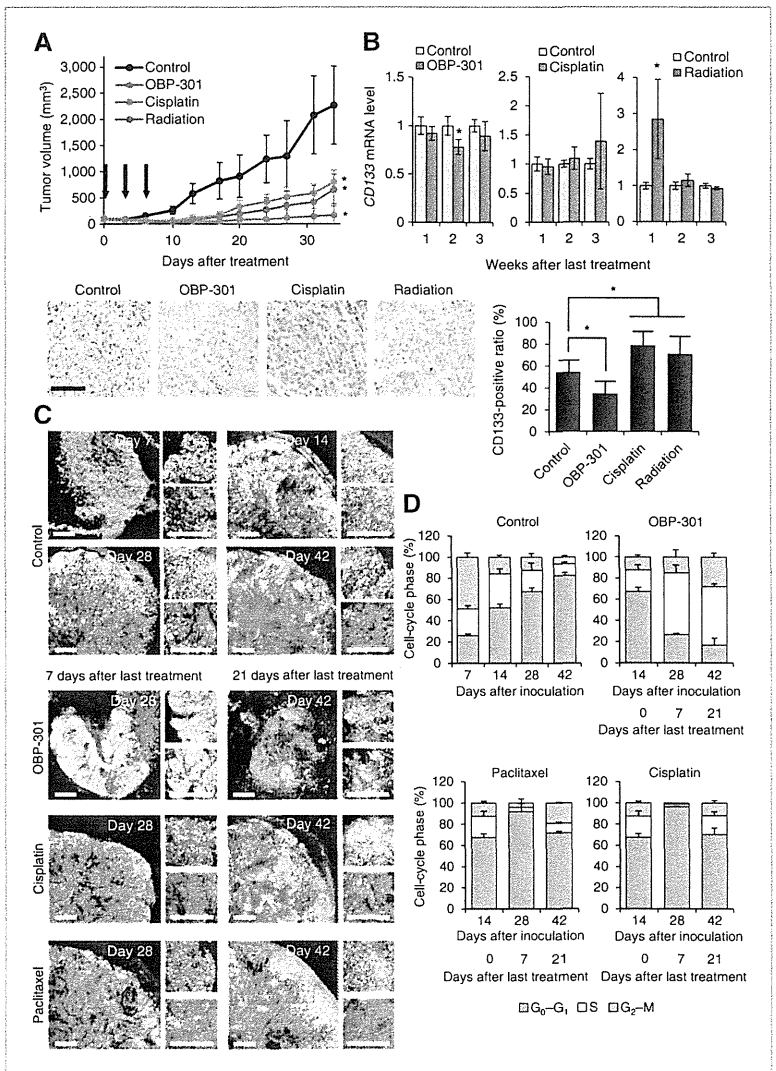

Figure 5. OBP-301 induces cell-cycle progression and efficiently kills dormant cancer cells resistant to conventional therapy in established human tumor xenografts. $CD133^+$-rich radioresistant MKN45 cells (5×10^6 cells/mouse) were injected subcutaneously into the left flanks of mice. When the tumors reached approximately 6 mm in diameter (tumor volume, 100–120 mm^3), mice were administered OBP-301 intratumorally (1×10^8 PFU/tumor), injected intraperitoneally with cisplatin (4 mg/kg), or exposed to 2 Gy of radiation for 3 cycles every 3 days. A, growth curves of tumors derived from radioresistant MKN45 cells after treatment with OBP-301, cisplatin or radiation. Black arrows indicate the day of treatment. B, expression of *CD133* mRNA in tumors treated with OBP-301, cisplatin, or radiation at 1, 2, and 3 weeks after treatment (top). Representative images of CD133-stained tumor section treated with OBP-301, cisplatin, or radiation (bottom left). Scale bars, 100 μm. Histogram shows the percentages of $CD133^-$ cells in tumors treated with OBP-301, cisplatin, or radiation (bottom right). The percentage of $CD133^+$ cells was calculated by dividing the number of $CD133^+$ cells by the total number of cells. Data are shown as means ± SD ($n = 3$). *, $P < 0.05$. C and D, FUCCI-expressing MKN45 cells (5×10^6 cells/mouse) were injected subcutaneously into the left flanks of mice. When the tumors reached approximately 7 mm in diameter (tumor volume, 150–180 mm^3), mice were administered OBP-301 intratumorally (1×10^8 PFU/tumor), injected intraperitoneally with cisplatin (4 mg/kg) or paclitaxel (5 mg/kg) for 3 cycles every 3 days. Representative images of cross-sections of FUCCI-expressing MKN45 subcutaneous tumors of control, OBP-301-, cisplatin-, or paclitaxel-treated mice (left). The cells in G_0–G_1, S, or G_2–M phases appear red, yellow, or green, respectively. Histogram shows the cell-cycle phase of FUCCI-expressing MKN45 subcutaneous tumor from control, OBP-301-, cisplatin-, or paclitaxel-treated mice (right). The percentage of cells in G_0–G_1, S, and G_2–M phases are shown. Data are shown as means ± SD ($n = 5$). *, $P < 0.05$. Scale bars, 500 μm.

Published OnlineFirst September 30, 2013; DOI: 10.1158/1078-0432.CCR-13-0742

After cisplatin or paclitaxel treatment, the tumor consisted mostly of red fluorescent cells (Fig. 5D), indicating that the cytotoxic agents killed only cycling cancer cells and had little effect on quiescent dormant cancer cells. These tumors regrew, with the quiescent cells re-entering the cell cycle 21 days after last treatment (Fig. 5D). In contrast, intratumor injection of OBP-301 mobilized the cancer cells into the S/G_2/M phase trap, leading to elimination of cancer cells in S/G_2/M phases (Fig. 5D). These data indicate that OBP-301 could efficiently kill quiescent cancer stem–like cells in tumors by inducing cell-cycle progression.

OBP-301 sensitizes quiescent cancer stem–like cells to chemotherapy by cell-cycle mobilization and S/G_2/M phase trapping

As we previously showed that OBP-301 enhances the sensitivities to chemotherapeutic agents in various types of human cancer cells (30, 31), we further evaluated whether OBP-301 sensitizes quiescent $CD133^+$ cancer stem–like cells to chemotherapy by inducing cell-cycle progression and S/G_2/M phase trapping. OBP-301 infection significantly enhanced the inhibitory effect of chemotherapy on cell viability and tumor sphere formation of $CD133^+$ cells (Fig. 6A and Supplementary

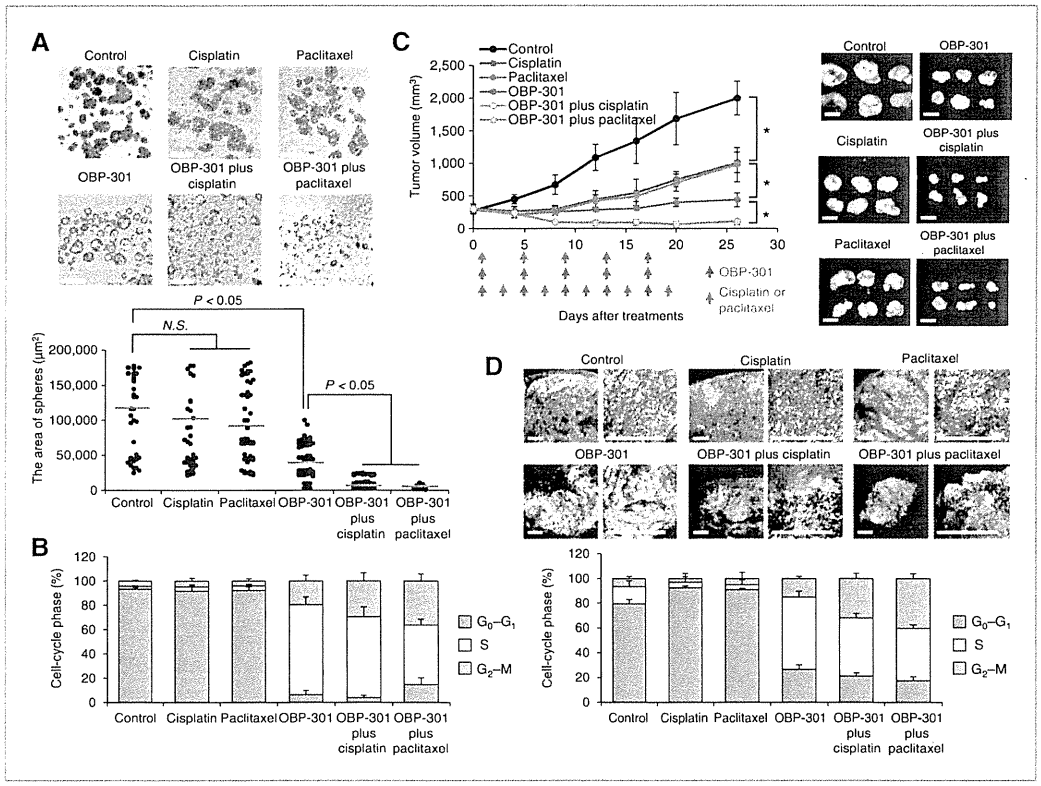

Figure 6. OBP-301 sensitizes quiescent $CD133^+$ cancer stem–like cells to chemotherapy by inducing cell-cycle progression. A, representative images of tumor spheres from FUCCI-expressing $CD133^+$ cells after treatment with cisplatin, paclitaxel, OBP-301, and the combination of OBP-301 and chemotherapy (top). The cells in G_0–G_1, S, or G_2–M phases appear red, yellow, or green, respectively. The tumor-sphere area was calculated using NIH ImageJ software (lower). Data are shown as means ± SD ($n = 5$). *, $P < 0.05$. Scale bars, 500 μm. B, histogram shows the cell-cycle phase of tumor spheres from FUCCI-expressing $CD133^+$ cells after treatment with chemotherapy, OBP-301, and the combination of OBP-301 and chemotherapy. The percentage of cells in G_0–G_1, S, and G_2–M phases are shown. Data are shown as means ± SD ($n = 5$). *, $P < 0.05$. C, FUCCI-expressing MKN45 cells (5×10^6 cells/mouse) were injected subcutaneously into the left flanks of mice. When the tumors reached approximately 8 mm in diameter (tumor volume, 300 mm^3), mice were administered OBP-301 intratumorally (1×10^8 PFU/tumor), injected intraperitoneally with cisplatin (4 mg/kg) or paclitaxel (5 mg/kg) for 5 cycles every 3 days. The growth curves of tumors derived from FUCCI-expressing MKN45 cells after treatment with chemotherapy, OBP-301, or the combination of OBP-301 and chemotherapy (left). Red and green arrows indicate the day of treatment with OBP-301 and chemotherapy, respectively. Macroscopic photographs of FUCCI-expressing tumors in untreated (control) or treated with OBP-301, cisplatin, paclitaxel, or the combination of OBP-301 and chemotherapy (right). Scale bars, 10 mm. D, representative image of cross-sections of FUCCI-expressing MKN45 subcutaneous tumors of control, OBP-301-, cisplatin-, paclitaxel-, or the combination of OBP-301- and chemotherapy-treated mice (top). Histogram shows cell-cycle phase of FUCCI-expressing MKN45 subcutaneous tumors of control, treated with OBP-301, cisplatin, paclitaxel, or the combination of OBP-301 and chemotherapy (bottom). Data are shown as means ± SD ($n = 6$). *, $P < 0.05$, ANOVA. Scale bars, 500 μm.

Published OnlineFirst September 30, 2013; DOI: 10.1158/1078-0432.CCR-13-0742

Fig. S13). Tumor spheres treated with chemotherapy and OBP-301 contained an increased percentage of tumor cells in G_2–M phases compared to OBP-301 alone (Fig. 6B). The combination of OBP-301 and chemotherapy (Supplementary Fig. S10C) significantly suppressed tumor growth compared to chemotherapy or OBP-301 alone (Fig. 6C and Supplementary Fig. S14). Cross-sections of tumor tissues showed that the combination of chemotherapy and OBP-301 induced an increased percentage of cancer cells in G_2–M phases compared to OBP-301 alone (Fig. 6D). These results suggest that OBP-301 sensitizes the quiescent cancer stem–like cells to chemotherapy-mediated G_2–M arrest by inducing cell-cycle progression and S/G_2/M phase trapping.

Discussion

We have described that a bioengineered telomerase-specific oncolytic adenovirus, OBP-301, efficiently kills $CD133^+$ cancer stem–like cells that have elevated telomerase activity through enhanced E1A-mediated cell-cycle mobilization and S-phase trapping. By using FUCCI technology in combination with tumor sphere culture, we visualized virus penetration, cell-cycle dynamics, and the subsequent elimination of quiescent cancer stem–like cells in dormant tumor spheres (Supplementary Fig. S15A).

Cancer stem–like cells have been shown to be highly resistant to chemotherapeutic agents (32, 33) and ionizing radiation (24–26). As expected, $CD133^+$ human gastric cancer cells were more resistant to conventional therapies than $CD133^-$ cells; OBP-301, however, efficiently reduced the viability of $CD133^+$ cells, similar to their reduction of viability of $CD133^-$ cells. Moreover, we showed that OBP-301 significantly reduced the stem cell properties of $CD133^+$ cells *in vitro* and *in vivo* compared with conventional chemoradiotherapy and further sensitized $CD133^+$ cancer stem–like cells to chemotherapy. These findings indicate that OBP-301 is a promising anticancer therapy to eliminate cancer stem–like cells more efficiently than conventional therapy in the clinical setting.

Recent studies have showed that p53 and $p21^{cip1/waf1}$ maintain the quiescent state in hematopoietic stem cells (34, 35). Moreover, $p27^{kip1}$ has been suggested to be involved in suppression of the transition from the G_0 phase to G_1–S phases (36, 37). Cancer stem–like cells maintain a more quiescent state than non–cancer stem–like cells, which is associated with cancer stem–like cell resistance to conventional therapies (9, 10). OBP-301 induced S and G_2–M phase entry and subsequent cell death in quiescent $CD133^+$ cells through upregulation of E2F1-related proteins and downregulation of p53-related and p27 proteins in an E1A-dependent manner. A recent report suggested that suppression of the p53-mediated G_1 checkpoint is required for E2F1-induced S-phase entry (38). Furthermore, adenoviral E1A has been shown to suppress p53-mediated cell-cycle arrest after DNA damage (39). Thus, OBP-301 can inhibit cancer stem–like cells from maintaining a quiescent state and force them into cycling by not only upregulating E2F-related proteins but also downregulating p53-related and p27 proteins (Supplementary Fig. S15B), leading to the sensitization to chemotherapy.

FUCCI (23) is a powerful tool to visualize the quiescent state in cancer stem–like cells and the treatment dynamics of OBP-301. When tumor spheres were formed, $CD133^+$ cells maintained a quiescent state, which was defined by red fluorescent nuclei expressed in G_0–G_1 phases. In contrast, S and G_2–M phase entry induced by OBP-301 could be clearly visualized as yellow and green fluorescent nuclei, respectively. Our data indicate that 3-dimensional cultures are extremely important for the maintenance of the quiescence of $CD133^+$ cells. FUCCI-based real-time imaging of the cell cycle provides a platform for the screening of candidate therapeutic agents that modulate the quiescent state of drug-resistant cancer stem–like cells.

In conclusion, we have clearly shown that a genetically-engineered oncolytic adenovirus, OBP-301, efficiently eradicates quiescent cancer stem–like cells in solid tumors by cell-cycle mobilization and S/G_2/M phase trapping. A phase I clinical trial of intratumoral injection of OBP-301 in patients with advanced solid tumors was recently completed and OBP-301 monotherapy was well tolerated by these patients (20). However, the difficulty of adenoviral delivery to inaccessible primary and metastatic tumor tissues is a major obstacle for clinical translation of this treatment modality. In this study, the combination therapy of OBP-301 with chemotherapy was highly effective antitumor therapy to eliminate both cancer stem–like and non–cancer stem–like cells in a xenograft model. Future clinical trials of intratumoral injection of OBP-301 in combination with conventional antitumor therapy are suggested by the results of the present study.

Disclosure of Potential Conflicts of Interest

Y. Urata is President & CEO of Oncolys BioPharma, Inc., the manufacturer of OBP-301 (Telomelysin). H. Tazawa and T. Fujiwara are consultants of Oncolys BioPharma, Inc. No potential conflicts of interest were disclosed by the other authors.

Authors' Contributions

Conception and design: S. Yano, H. Tazawa, R. M. Hoffman, T. Fujiwara
Development of methodology: S. Yano, H. Tazawa, Y. Hashimoto, S. Kuroda, H. Kishimoto
Acquisition of data (provided animals, provided facilities, etc): S. Yano, H. Tazawa, Y. Hashimoto
Analysis and interpretation of data (e.g., statistical analysis, biostatistics, computational analysis): S. Yano, H. Tazawa, Y. Hashimoto, Nagasaka, S. Kagawa, T. Fujiwara
Writing, review, and/or revision of manuscript: S. Yano, H. Tazawa, R. M. Hoffman, T. Fujiwara
Administrative, technical, or material support: Y. Urata, R. M. Hoffman
Study supervision: H. Tazawa, Y. Shirakawa, M. Nishizaki, T. Nagasaka, S. Kagawa, R. M. Hoffman, T. Fujiwara

Acknowledgments

The authors thank Yukinari Isomoto and Tomoko Sueishi for their technical support.

Published OnlineFirst September 30, 2013; DOI: 10.1158/1078-0432.CCR-13-0742

Grant Support

This work was supported, in part, by grants from the Ministry of Education, Culture, Sports, Science, and Technology of Japan (to T. Fujiwara, No. 22390256) and by grants from the Ministry of Health, Labour, and Welfare of Japan (to T. Fujiwara, No. 10103827, No. 09156285).

The costs of publication of this article were defrayed in part by the payment of page charges. This article must therefore be hereby marked *advertisement* in accordance with 18 U.S.C. Section 1734 solely to indicate this fact.

Received March 20, 2013; revised September 10, 2013; accepted September 10, 2013; published OnlineFirst September 30, 2013.

References

1. Goss PE, Chambers AF. Does tumour dormancy offer a therapeutic target? Nat Rev Cancer 2010;10:871–7.
2. Aguirre-Ghiso JA. Models, mechanisms and clinical evidence for cancer dormancy. Nat Rev Cancer 2007;7:834–46.
3. Reya T, Morrison SJ, Clarke MF, Weissman IL. Stem cells, cancer, and cancer stem cells. Nature 2001;414:105–11.
4. Pardal R, Clarke MF, Morrison SJ. Applying the principles of stem-cell biology to cancer. Nat Rev Cancer 2003;3:895–902.
5. Clarke MF, Dick JE, Dirks PB, Eaves CJ, Jamieson CH, Jones DL, et al. Cancer stem cells–perspectives on current status and future directions: AACR Workshop on cancer stem cells. Cancer Res 2006;66:9339–44.
6. Visvader JE, Lindeman GJ. Cancer stem cells in solid tumours: accumulating evidence and unresolved questions. Nat Rev Cancer 2008;8:755–68.
7. Trumpp A, Wiestler OD. Mechanisms of Disease: cancer stem cells–targeting the evil twin. Nat Clin Pract Oncol 2008;5:337–47.
8. Zhou BB, Zhang H, Damelin M, Geles KG, Grindley JC, Dirks PB. Tumour-initiating cells: challenges and opportunities for anticancer drug discovery. Nat Rev Drug Discov 2009;8:806–23.
9. Ito K, Bernardi R, Morotti A, Matsuoka S, Saglio G, Ikeda Y, et al. PML targeting eradicates quiescent leukaemia-initiating cells. Nature 2008;453:1072–8.
10. Saito Y, Uchida N, Tanaka S, Suzuki N, Tomizawa-Murasawa M, Sone A, et al. Induction of cell cycle entry eliminates human leukemia stem cells in a mouse model of AML. Nat Biotechnol 2010;28:275–80.
11. Alemany R, Balague C, Curiel DT. Replicative adenoviruses for cancer therapy. Nat Biotechnol 2000;18:723–7.
12. Russell SJ, Peng KW, Bell JC. Oncolytic virotherapy. Nat Biotechnol 2012;30:658–70.
13. Stracker TH, Carson CT, Weitzman MD. Adenovirus oncoproteins inactivate the Mre11-Rad50-NBS1 DNA repair complex. Nature 2002;418:348–52.
14. Flinterman M, Gaken J, Farzaneh F, Tavassoli M. E1A-mediated suppression of EGFR expression and induction of apoptosis in head and neck squamous carcinoma cell lines. Oncogene 2003;22:1965–77.
15. Yu D, Wolf JK, Scanlon M, Price JE, Hung MC. Enhanced c-erbB-2/neu expression in human ovarian cancer cells correlates with more severe malignancy that can be suppressed by E1A. Cancer Res 1993;53:891–8.
16. Eriksson M, Guse K, Bauerschmitz G, Virkkunen P, Tarkkanen M, Tanner M, et al. Oncolytic adenoviruses kill breast cancer initiating CD44+CD24-/low cells. Mol Ther 2007;15:2088–93.
17. Zhang X, Komaki R, Wang L, Fang B, Chang JY. Treatment of radioresistant stem-like esophageal cancer cells by an apoptotic gene-armed, telomerase-specific oncolytic adenovirus. Clin Cancer Res 2008;14:2813–23.
18. Kanai R, Rabkin SD, Yip S, Sgubin D, Zaupa CM, Hirose Y, et al. Oncolytic virus-mediated manipulation of DNA damage responses: synergy with chemotherapy in killing glioblastoma stem cells. J Natl Cancer Inst 2012;104:42–55.
19. Kawashima T, Kagawa S, Kobayashi N, Shirakiya Y, Umeoka T, Teraishi F, et al. Telomerase-specific replication-selective virotherapy for human cancer. Clin Cancer Res 2004;10:285–92.
20. Nemunaitis J, Tong AW, Nemunaitis M, Senzer N, Phadke AP, Bedell C, et al. A phase I study of telomerase-specific replication competent oncolytic adenovirus (telomelysin) for various solid tumors. Mol Ther 2010;18:429–34.
21. Yokozaki H. Molecular characteristics of eight gastric cancer cell lines established in Japan. Pathol Int 2000;50:767–77.
22. Hashimoto Y, Watanabe Y, Shirakiya Y, Uno F, Kagawa S, Kawamura H, et al. Establishment of biological and pharmacokinetic assays of telomerase-specific replication-selective adenovirus. Cancer Sci 2008;99:385–90.
23. Sakaue-Sawano A, Kurokawa H, Morimura T, Hanyu A, Hama H, Osawa H, et al. Visualizing spatiotemporal dynamics of multicellular cell-cycle progression. Cell 2008;132:487–98.
24. Baumann M, Krause M, Hill R. Exploring the role of cancer stem cells in radioresistance. Nat Rev Cancer 2008;8:545–54.
25. Bao S, Wu Q, McLendon RE, Hao Y, Shi Q, Hjelmeland AB, et al. Glioma stem cells promote radioresistance by preferential activation of the DNA damage response. Nature 2006;444:756–60.
26. Phillips TM, McBride WH, Pajonk F. The response of CD24(−/low)/CD44 +breast cancer-initiating cells to radiation. J Natl Cancer Inst 2006;98:1777–85.
27. Nakayama KI, Nakayama K. Ubiquitin ligases: cell-cycle control and cancer. Nat Rev Cancer 2006;6:369–81.
28. Lee J, Kotliarova S, Kotliarov Y, Li A, Su Q, Donin NM, et al. Tumor stem cells derived from glioblastomas cultured in bFGF and EGF more closely mirror the phenotype and genotype of primary tumors than do serum-cultured cell lines. Cancer Cell 2006;9:391–403.
29. Ricci-Vitiani L, Lombardi DG, Pilozzi E, Biffoni M, Todaro M, Peschle C, et al. Identification and expansion of human colon-cancer-initiating cells. Nature 2007;445:111–5.
30. Fujiwara T, Kagawa S, Kishimoto H, Endo Y, Hioki M, Ikeda Y, et al. Enhanced antitumor efficacy of telomerase-selective oncolytic adenoviral agent OBP-401 with docetaxel: preclinical evaluation of chemovirotherapy. Int J Cancer 2006;119:432–40.
31. Liu D, Kojima T, Ouchi M, Kuroda S, Watanabe Y, Hashimoto Y, et al. Preclinical evaluation of synergistic effect of telomerase-specific oncolytic virotherapy and gemcitabine for human lung cancer. Mol Cancer Ther 2009;8:980–7.
32. Dean M, Fojo T, Bates S. Tumour stem cells and drug resistance. Nat Rev Cancer 2005;5:275–84.
33. Ma S, Lee TK, Zheng BJ, Chan KW, Guan XY. CD133+ HCC cancer stem cells confer chemoresistance by preferential expression of the Akt/PKB survival pathway. Oncogene 2008;27:1749–58.
34. Cheng T, Rodrigues N, Shen H, Yang Y, Dombkowski D, Sykes M, et al. Hematopoietic stem cell quiescence maintained by p21cip1/waf1. Science 2000;287:1804–8.
35. Liu Y, Elf SE, Miyata Y, Sashida G, Huang G, Di Giandomenico S, et al. p53 regulates hematopoietic stem cell quiescence. Cell Stem Cell 2009;4:37–48.
36. Sutterluty H, Chatelain E, Marti A, Wirbelauer C, Senften M, Muller U, et al. p45SKP2 promotes p27Kip1 degradation and induces S phase in quiescent cells. Nat Cell Biol 1999;1:207–14.
37. Kamura T, Hara T, Matsumoto M, Ishida N, Okumura F, Hatakeyama S, et al. Cytoplasmic ubiquitin ligase KPC regulates proteolysis of p27 (Kip1) at G1 phase. Nat Cell Biol 2004;6:1229–35.
38. Lomazzi M, Moroni MC, Jensen MR, Frittoli E, Helin K. Suppression of the p53- or pRB-mediated G1 checkpoint is required for E2F-induced S-phase entry. Nat Genet 2002;31:190–4.
39. Steegenga WT, van Laar T, Riteco N, Mandarino A, Shvarts A, van der Eb AJ, et al. Adenovirus E1A proteins inhibit activation of transcription by p53. Mol Cell Biol 1996;16:2101–9.

The hTERT Promoter Enhances the Antitumor Activity of an Oncolytic Adenovirus under a Hypoxic Microenvironment

Yuuri Hashimoto[1], Hiroshi Tazawa[1,2], Fuminori Teraishi[1], Toru Kojima[1], Yuichi Watanabe[1], Futoshi Uno[1], Shuya Yano[1], Yasuo Urata[3], Shunsuke Kagawa[1], Toshiyoshi Fujiwara[1]*

1 Department of Gastroenterological Surgery, Graduate School of Medicine, Dentistry and Pharmaceutical Sciences, Okayama University, Okayama, Japan, **2** Center for Gene and Cell Therapy, Okayama University Hospital, Okayama, Japan, **3** Oncolys BioPharma, Inc., Tokyo, Japan

Abstract

Hypoxia is a microenvironmental factor that contributes to the invasion, progression and metastasis of tumor cells. Hypoxic tumor cells often show more resistance to conventional chemoradiotherapy than normoxic tumor cells, suggesting the requirement of novel antitumor therapies to efficiently eliminate the hypoxic tumor cells. We previously generated a tumor-specific replication-competent oncolytic adenovirus (OBP-301: Telomelysin), in which the human telomerase reverse transcriptase (*hTERT*) promoter drives viral E1 expression. Since the promoter activity of the *hTERT* gene has been shown to be upregulated by hypoxia, we hypothesized that, under hypoxic conditions, the antitumor effect of OBP-301 with the *hTERT* promoter would be more efficient than that of the wild-type adenovirus 5 (Ad5). In this study, we investigated the antitumor effects of OBP-301 and Ad5 against human cancer cells under a normoxic (20% oxygen) or a hypoxic (1% oxygen) condition. Hypoxic condition induced nuclear accumulation of the hypoxia-inducible factor-1α and upregulation of *hTERT* promoter activity in human cancer cells. The cytopathic activity of OBP-301 was significantly higher than that of Ad5 under hypoxic condition. Consistent with their cytopathic activity, the replication of OBP-301 was significantly higher than that of Ad5 under the hypoxic condition. OBP-301-mediated E1A was expressed within hypoxic areas of human xenograft tumors in mice. These results suggest that the cytopathic activity of OBP-301 against hypoxic tumor cells is mediated through hypoxia-mediated activation of the *hTERT* promoter. Regulation of oncolytic adenoviruses by the *hTERT* promoter is a promising antitumor strategy, not only for induction of tumor-specific oncolysis, but also for efficient elimination of hypoxic tumor cells.

Citation: Hashimoto Y, Tazawa H, Teraishi F, Kojima T, Watanabe Y, et al. (2012) The hTERT Promoter Enhances the Antitumor Activity of an Oncolytic Adenovirus under a Hypoxic Microenvironment. PLoS ONE 7(6): e39292. doi:10.1371/journal.pone.0039292

Editor: Ilya Ulasov, University of Chicago, United States of America

Received November 10, 2011; **Accepted** May 18, 2012; **Published** June 15, 2012

Funding: This work was supported in part by grants from the Ministry of Education, Culture, Sports, Science and Technology of Japan (to TF and FT, http://www.mext.go.jp/english/) and by grants from the Ministry of Health, Labour and Welfare of Japan (to TF, http://www.mhlw.go.jp/english/). The funders had no role in study design, data collection and analysis, decision to publish, or preparation of the manuscript.

Competing Interests: YU is an employee of Oncolys BioPharma, Inc., the manufacturer of OBP-301. TF is a consultant of Oncolys BioPharma, Inc. This does not alter the authors' adherence to all the PLoS ONE policies on sharing data and materials.

* E-mail: toshi_f@md.okayama-u.ac.jp

Introduction

Solid tumor tissues often contain hypoxic regions, in which the supply of oxygen and nutrition is reduced because of an immature vascular network, and in which there is rapid tumor progression [1]. Hypoxia is a critical microenvironmental factor that contributes to tumor angiogenesis, invasion, progression and metastasis [1,2]. Indeed, hypoxic conditions have been shown to be associated with cancer progression and poor prognosis [3–5]. Furthermore, recent accumulated evidence suggests that hypoxia induces cancer progression-related characteristics such as epithelial-mesenchymal transition (EMT) [6,7] and stemness properties [8–11] of tumor cells. Acquisition of such properties by tumor cells within hypoxic areas of tumor tissues would greatly contribute to tumor progression and recurrence.

Hypoxic tumor cells are known to be highly resistant to conventional chemoradiotherapy, leading to poor prognosis [5,12]. To improve clinical outcome, novel antitumor agents that efficiently eradicate tumor cells under hypoxic conditions as well as under normoxic conditions are required. Oncolytic virotherapy has emerged as a promising novel antitumor therapy [13]. We previously generated a telomerase-specific replication-competent oncolytic adenovirus (OBP-301: Telomelysin), in which the human telomerase reverse transcriptase (*hTERT*) promoter element drives E1 gene expression. OBP-301 efficiently kills human cancer cells but not normal human somatic cells [14]. hTERT is a catalytic subunit of human telomerase and is highly expressed in tumor cells, but not in normal cells. hTERT expression closely correlates with telomerase activity [15–17]. Tumor-specific antitumor activity of OBP-301 against various types of human cancer cells with high telomerase activity has been demonstrated in both *in vitro* and *in vivo* settings [14,18,19]. Furthermore, the feasibility of OBP-301 for clinical use has been demonstrated in a recently completed phase I clinical trial in the USA of OBP-301 in patients with advanced solid tumors [20]. However, whether OBP-301 has an antitumor effect against hypoxic tumor cells remains unclear.

Hypoxia-inducible factor 1 (HIF-1) is a master transcription factor that is activated by hypoxia [1]. HIF-1 consists of α and β subunits and HIF-1α expression is tightly regulated by oxygen concentration. The HIF-1α protein is stabilized under hypoxic conditions, whereas it is immediately degraded under normoxic conditions. HIF-1α induces the expression of many down-stream target genes that are associated with cellular metabolism, proliferation, survival, apoptosis, neovascularization and migration [4]. The expression of many target genes is activated by HIF-1 through binding to a *cis*-acting hypoxia response element (HRE) located at their enhancer or promoter regions [4,21,22]. The *hTERT* gene is also a HIF-1-target gene. Two HREs that are present in the *hTERT* gene promoter are involved in hypoxia-mediated *hTERT* gene upregulation [23–25]. In contrast, it has also been shown that hypoxic conditions impair the replication of wild-type adenovirus in tumor cells [26,27]. Based on these findings, we hypothesized that the cytopathic activity of OBP-301 that is regulated by the *hTERT* gene promoter would be much stronger against hypoxic tumor cells than that of wild-type adenovirus due to hypoxia-induced enhancement of OBP-301 virus replication.

In the present study, we evaluated whether hypoxic conditions affect the expression levels of hTERT and the coxsackie and adenovirus receptor (CAR) in human cancer cells. We next assessed the antitumor effects of OBP-301 and Ad5 against human cancer cells under normoxic or hypoxic conditions. We further evaluated the replication of OBP-301 within hypoxic areas of human xenograft tumors.

Results

Maintenance of human cancer cells under hypoxic conditions

A hypoxia chamber filled with a gas mixture of 1% O_2, 5% CO_2 and 94% N_2 was used to maintain human cancer cells under hypoxic conditions. Human cancer cells were also maintained under normoxic conditions, consisting of 20% O_2 and 5% CO_2. To first confirm that the tumor cells were efficiently exposed to hypoxia in the chamber, the expression of HIF-1α, which is the main transcription factor induced by hypoxia [1], was evaluated using Western blot analysis. Consistent with HIF-1α induction by exposure to cobalt chloride ($CoCl_2$), HIF-1α expression was strongly induced in human cancer cells (HT29, DLD-1, H1299) maintained in the hypoxia chamber (Fig. 1A). However, no, or slight, HIF-1α expression was detected under normoxic conditions. Moreover, using immunocytochemistry, we further confirmed that HIF-1α was expressed and accumulated in the nuclei of human cancer cells under hypoxic conditions, but not under normoxic conditions (Fig. 1B). These results indicate that human cancer cells are maintained under hypoxic conditions in the hypoxia chamber.

Expression of hTERT and the adenovirus receptor in human cancer cells under hypoxic conditions

OBP-301 contains the *hTERT* gene promoter, which allows tumor-specific regulation of the gene expression of *E1A* and *E1B* that are required for viral replication [14]. The activity of the *hTERT* gene promoter in human cancer cells has been shown to be upregulated under hypoxic conditions [23–25], suggesting that hypoxia would enhance OBP-301 replication through upregulation of *hTERT* gene promoter activity. To evaluate the effect of hypoxic conditions on the activity of the *hTERT* gene promoter in tumor cells, we first investigated the expression level of *hTERT* mRNA in human tumor cells under normoxic or hypoxic conditions by quantitative real-time RT-PCR analysis. The expression of *hTERT* mRNA was increased in all tumor cells under the hypoxic condition by 1.3 to 4.3-fold compared to the normoxic condition (Fig. 2A). Despite evident inductions of HIF-1α by hypoxia, the increases were not statistically significant in HT29 and DLD-1 cells. Because it is known that hTERT expression is regulated not only transcriptionally but also post-transcriptionally by alternative splicing [25], we further examined the effects of hypoxia on activity of exogenous *hTERT* gene promoter using luciferase reporter assay. Hypoxia activated the *hTERT* gene promoter by at least 3-fold compared to the *hTERT* gene promoter activity under normoxia (Fig. 2B). To further confirm hypoxia-induced *hTERT* promoter activation, we used chemical inhibitor of HIF-1α. The protein expression of HIF-1α and the activity of *hTERT* gene promoter were significantly decreased in HT29 and H1299 cells treated with 30 μM HIF-1α inhibitor LW6 and cultured in hypoxic condition (Fig. S1 and Fig. 2C). Moreover, we confirmed that hTERT protein was expressed and accumulated in nuclei of human cancer cells under hypoxic conditions by immunofluorescence staining (Fig. 2D). These results suggest that the *hTERT* gene promoter in OBP-301 is more strongly activated under the hypoxic condition than under the normoxic condition.

The infection efficiency of Ad5-based viral vectors depends mainly on the expression of the adenoviral receptor CAR in target cells [28]. Therefore, to evaluate whether hypoxic conditions affect the expression of CAR in tumor cells, we examined the expression level of CAR in all tumor cells under normoxic or hypoxic conditions by flow cytometry. CAR expression was clearly detected in all tumor cells tested: the percentage of CAR-positive cells was 99.5%, 99.3% and 98.8% for HT29, DLD-1 and H1299 cells, respectively (Fig. 2E). All tumor cell lines showed similar expression levels of CAR under normoxic and hypoxic conditions. These results indicate that tumor cells show high CAR expression under hypoxic conditions as well as under normoxic conditions.

Antitumor activities of OBP-301 and Ad5 against hypoxic tumor cells

To explore the potential antitumor activities of the telomerase-dependent oncolytic adenovirus OBP-301 against normoxic and hypoxic tumor cells, we investigated the cytopathic activities of OBP-301 and Ad5 against tumor cells under normoxic or hypoxic conditions. Under normoxic conditions, the cytopathic activities of OBP-301 and Ad5 against HT29 and DLD-1 cells were very similar. The cytopathic activity of OBP-301 against H1299 cells was significantly higher than that of Ad5 at a low dose of infection, whereas it was similar to that of Ad5 at a high dose of infection (Fig. 3A). In contrast, under hypoxic conditions, the cytopathic activity of OBP-301 against all tumor cells was significantly higher than that of Ad5, especially at a high dose of infection (Fig. 3B). To further evaluate the antitumor activities of OBP-301 and Ad5 against hypoxic tumor cells, the 50% inhibiting dose (ID_{50}) values of OBP-301 and Ad5 under a hypoxic or a normoxic condition were calculated. The calculated ID_{50} values indicated that the cytopathic activity of OBP-301 against all tumor cells under hypoxic conditions was higher than that of Ad5, although the cytopathic activities of OBP-301 and Ad5 were very similar under normoxic conditions (Table 1). These results suggest that the cytopathic activity of OBP-301 against hypoxic tumor cells is more efficient than that of Ad5.

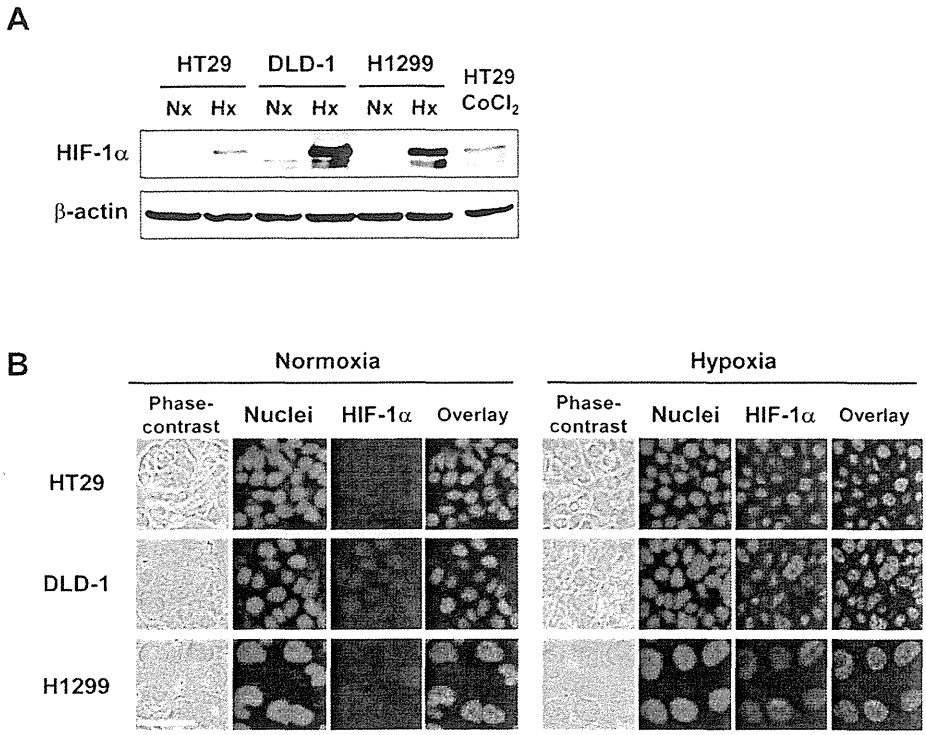

Figure 1. Increased HIF-1α expression in human cancer cells under hypoxic conditions. A, Western blot analysis of HIF-1α protein expression in human cancer cells (HT29, DLD-1 and H1299) under normoxic (Nx) or hypoxic (Hx) conditions. Cells were maintained under a normoxic (20% O_2) or a hypoxic (1% O_2) condition for 18 h. HT29 cells were also exposed to $CoCl_2$ as a positive control. Cell lysates were subjected to Western blot analysis using an anti- HIF-1α antibody. β-actin was assayed as a loading control. **B,** Subcellular localization of HIF-1α expression in human cancer cells under normoxia or hypoxia was assessed using immunofluorescent staining. Cells cultured under a normoxic or a hypoxic condition for 18 h were stained with anti-HIF-1α antibody (red). Nuclei were counterstained with DAPI (blue). Scale bars = 50 μm.
doi:10.1371/journal.pone.0039292.g001

Increased replication of OBP-301 compared to that of Ad5 under hypoxic conditions

We next examined the ability of OBP-301 and Ad5 to replicate in HT29, DLD-1 and H1299 cells, which showed almost similar sensitivity to OBP-301 and Ad5 under normoxic conditions but different sensitivity under hypoxic conditions (Fig. 3). The replication ability of OBP-301 and Ad5 was quantified by measuring viral E1A DNA in tumor cells infected with OBP-301 or Ad5 using quantitative real-time PCR analysis. Under normoxic conditions, the amount of virus production was very similar in tumor cells after infection with OBP-301 or Ad5 (Fig. 4). In contrast, under hypoxic conditions, viral production was significantly increased in OBP-301-infected tumor cells compared to Ad5-infected cells (Fig. 4). These results suggest that the replication of OBP-301 within hypoxic tumor cells is more efficient than that of Ad5.

OBP-301-mediated E1A expression in the hypoxic regions of xenograft tumor tissues

To investigate whether OBP-301 actually replicates in the hypoxic regions of tumor tissues, we examined HT29 and DLD-1 xenograft tumors after intratumoral injection of OBP-301. OBP-301-mediated E1A protein expression was assessed in HT29 and DLD-1 xenograft tumors by immunohistochemistry. Hypoxic areas in tumor tissues were detected by immunohistochemical analysis of the exogenous hypoxic marker, pimonidazole hydrochloride. OBP-301-mediated E1A was expressed in the normoxic regions (Fig. 5Aa and 5Ba) and the regions that were confirmed to be hypoxic by detection of pimonidazole expression (Fig. 5Ab and 5Bb). Moreover, the quantitative image analysis of immunohistochemical stains showed that the E1A-positive areas were almost equal in pimonidazole-negative and pimonidazole-positive regions (Fig. 5C and 5D). These results suggest that OBP-301 replicates in hypoxic tumor cells within the hypoxic areas of tumor tissues.

Discussion

Hypoxic microenvironments contribute to tumor invasion, progression, metastasis and resistance to conventional antitumor therapy, such as chemotherapy and radiotherapy, leading to poor prognosis [1–5]. The development of novel antitumor therapies that efficiently eliminate hypoxic tumor cells is an urgent issue for improvement of the clinical outcome of cancer patients. Although adenovirus-based oncolytic virotherapy has recently emerged as a promising antitumor therapy, a hypoxic microenvironment has been shown to reduce the replication of wild-type adenovirus in target tumor cells [26,27]. Therefore, efficient replication of an oncolytic adenovirus under hypoxic conditions is a critical factor for the eradication of hypoxic tumor cells. In this study, our goal was to assess whether the telomerase-specific oncolytic adenovirus OBP-301 that is regulated by the *hTERT* gene promoter shows cytopathic activity against human tumor cells under hypoxic conditions. We demonstrated that the cytopathic activity of OBP-301 against hypoxic tumor cells was much stronger than that of wild-type adenovirus (Fig. 3 and Table 1). Hypoxia-mediated